WP4

Platy limestone as cultural heritage

Annex 3.2

Analysis of Platy Limestone Chemical and Mechanical Properties

Istrian Development Agency IDA d.o.o.

Tea Zubin Ferri

Pula, June 2015

The project is co-funded by the European Union
Instrument for Pre-Accession Assistance

REPUBLIC OF SLOVENIA
MINISTRY OF ECONOMIC DEVELOPMENT AND TECHNOLOGY

Table of Contents

Chemical characterization of platy limestone degradation typologies	**3**
Introduction	3
Aim of the research, samples and analysis methods description	3
Preliminary microscopic observations	8
Cross-sections preparation, optical microscopy, scanning electron microscopy and microanalysis (SEM/EDS) and infrared spectroscopy (FT-IR, µFT-IR)	**17**
Conclusions	39
Mechanical properties of platy limestone	**43**
Testing of flexural strength under constant moment	43
Testing of flexural strength under constant moment	45
Mercury intrusion porosimetry	46
Conclusions	51
Chemometric analysis of FT-IR spectra of platy limestone samples	**52**
Cluster analysis	53
Conclusions	58
References	59
Equipment list	59
Acknowledgements	59

Chemical characterization of platy limestone degradation typologies

Introduction

It is easy to recognize that stone has been a great witness of all the most important past civilizations, starting from the Neolithic tools to Egypt's pyramids, from the greek temples and theaters to the imperial roman fora, from the majestic gothic cathedrals until today's paving of our squares. To cope the passing of the centuries and the human negligence affecting this unreplaceable heritage, the knowledge of the collateral effects to this material is needed, if not crucial. Understanding the mechanism of degradation is essential in order to recognize and prevent them having in mind that the alteration that rocks undergo is just a transformation of the mineral matter caused by a disequilibrium existing between the environments in which the rocks are originated and the surface of the lithosphere. The set of physico-chemical reactions that occur between the lithosphere and the atmosphere on one side, the hydrosphere and the biosphere to the other, form the meteoric alteration (or evolution) of the rocks. These effects caused by external, climatic, factor have to be associated to those that are internal of the rock like its composition and structure which determine mechanical and chemical resistance and durability. The intensity and the rapidity of meteoric alteration depend on the combination of the factors mentioned above which have to be studied and treated together. According to the second law of thermodynamics, these alterations are considered as an irreversible natural phenomenon and considerations can be only made about the rapidity of the degradation process and its mechanisms. The technologies and methodologies available and applicable today in research regarding materials are multiple, very precise and efficient enabling us to study different aspects of the physic-chemical reactions occurring in materials of various typology, including rocks.

Aim of the research and methods description

The main aim of this study was to characterize the degradations that affect platy limestone in different location within the project area and to compare them with each other, to relate

them to the environment and to compare them with the degradation that occur on other limestone typologies, especially those that are located in urban areas. Since platy limestone was used mostly in rural areas, the composition of atmospheric deposition and patinas on the stone surface and their interaction with platy limestone mineral structure, were the aspects studied more in detail. Furthermore, platy limestone is characterized by an expressed stratified structure, which often origins exfoliations and material loss due to the detachment of portions of material in concomitance of these layer, present along the whole rock highness.

The present elaborate includes also the results of mechanical testing performed on platy limestone samples and the comparison of these values with those of other more well studied and diffused limestone typologies.

Finally, platy limestone represents an "unknown" material, which was practically left out of a systematic and detailed study and characterization. This occurred probably because it was mostly used in rural areas on rural building which, beside the ethnological and historical value, do not possess an artistic or architectonical value like the one we are used to when thinking about the monuments in our urban centers.

The analytic techniques used in this research for the chemical characterization are mostly microscopic and micro-spectroscopic which were applied using various methods:

- ✓ *Optical microscopy* – using visible, ultraviolet or polarized light
- ✓ *Electron microscopy* – with a scanning electron microscope and detectors for secondary and backscattered electrons, depending on the studied aspects (morphology or differences in composition) of each analyzed sample.
- ✓ *Fourier transform infrared spectroscopy* – sample preparation as pastilles, spectra interpretation and comparison with standards' spectra. Statistical chemometric analysis of obtained spectra.
- ✓ *Micro Fourier transform infrared spectroscopy* – FT-IR spectra acquisition directly on the cross-sections determining the composition of single layers (min. thickness 10 micrometers).

Mechanical properties of platy limestone were tested by measuring:

- ✓ *The flexural strength under constant moment*
- ✓ *The uniaxial compressive strength*
- ✓ *Mercury intrusion porosimetry*

The first two measurements have been performed according to the relative standards' prepositions (EN 1926:2007 and EN 13161:2008 respectively) using a static universal testing machine.

Using Fourier transform infrared spectroscopy (FT-IR), chemical composition of the bulk and the patinas of all the samples were studied. The FT-IR spectra collected were then used to implement a statistical analysis applying chemometric methods in order to define, if existing, similarity in chemical composition across platy limestone samples and to determine what the differences consist of, where found. The aim of this analysis was to correlate the sample composition to its location and to possibly find a similarity with samples taken nearby. Chemometric method used for the above explained purpose was:

- ✓ *Cluster analysis* – using standardized FT-IR spectra, Ward's algorithm for similarity calculations and Euclidean distance as metrics.

The results are represented as dendrograms, at the end of this elaborate.

SAMPLE LIST / Chemical analysis						
Ord. n.	Sample ID	Object	Description/ position	Partner/ External ex.	Country	Analysis implemented
1	ID 3300	Trogir - Cathedral	Roof of the south apse	RERA	CROATIA	FT-IR (B/P)
2	ID 3400	Grohote- Ruića Dvor	Roof	HGI	CROATIA	MS, OM, FT-IR (B/P)
3	ZAD 1	Roman sidewalk in Zadar	Sidewalk	Silvije Pranjić (ZADRA NOVA)	CROATIA	FT-IR (B/P)
4	ZAD 2	Austro-hungarian sidewalk- Zadar	Sidewalk	Silvije Pranjić (ZADRA NOVA)	CROATIA	FT-IR (B/P)
5	ZAD 3	Medviđa, sv. Ivan Krstitelj	Roof of the church	Silvije Pranjić (ZADRA NOVA)	CROATIA	MS, OM, µFT-IR, SEM/EDS
6	ZAD 4	Medviđa, sv. Ivan Krstitelj	Presbytery	Silvije Pranjić (ZADRA NOVA)	CROATIA	MS, OM, µFT-IR, SEM/EDS
7	ZAD 5	Medviđa, sv. Ivan Krstitelj	Sidewalk	Silvije Pranjić (ZADRA NOVA)	CROATIA	MS, OM, µFT-IR
8	ZAD 6	Ovča quarry – Dugi Otok	Sample from the quarry (not platy)	Silvije Pranjić (ZADRA NOVA)	CROATIA	FT-IR (B/P)
9	SLO1	Škrateljinova domačija, Divača	Roof	ZRS Koper	SLOVENIA	MS, OM, SEM/EDS
10	SLO2	Pri Blaževih	Roof	ZRS Koper	SLOVENIA	MS, OM, SEM/EDS
11	SLO3	Cerkev Marijinega vnebovzetja na Guri - Plešivica pri Povirju	Roof	ZRS Koper	SLOVENIA	FT-IR (B/P)
12	SLO4	Cerkev Marijinega vnebovzetja -Šmarje pri sežani	Roof	ZRS Koper	SLOVENIA	MS, OM, FT-IR (B/P)
13	SLO5	Cerkev Marijinega vnebovzetja- Šmarje pri sežani	Presbytery, wall below	ZRS Koper	SLOVENIA	MS, OM, µFT-IR
14	SLO6	Cerkev sv. Elije - Kopriva	Foundation	ZRS Koper	SLOVENIA	MS, OM, SEM/EDS
15	ITA 1	Trebiciano 107	Roof	diGEO- UNITS	ITALY	MS, OM, FT-IR (B/P)
16	ITA 2	Rupingrande 31	Roof	diGEO- UNITS	ITALY	MS, OM, FT-IR (B/P)
17	n. 1039	Basovizza – Kosovel 28	Roof	diGEO- UNITS	ITALY	MS, OM, FT-IR (B/P)
18	n. 1100	Rupinpiccolo 4	Roof	diGEO- UNITS	ITALY	MS, OM, FT-IR (B/P)
19	n. 1104	Rupinpiccolo 17	Roof	diGEO- UNITS	ITALY	MS, OM, FT-IR (B/P)
20	HR1	Franci	Quarry/outcrop	HGI	CROATIA	FT-IR (B/P)
21	HR2	Zrenj 1 ZR1	Quarry/outcrop	HGI	CROATIA	FT-IR (B/P)
22	HR3	Zrenj 2 ZR2	Quarry/outcrop	HGI	CROATIA	FT-IR (B/P)
23	HR4	Baderna	Quarry/outcrop	HGI	CROATIA	FT-IR (B/P)
24	HR5	Baderna 2	Quarry/outcrop	HGI	CROATIA	FT-IR (B/P)
25	HR6	Muzici	Quarry/outcrop	HGI	CROATIA	FT-IR (B/P)
26	HR7	Laganisi	Quarry/outcrop	HGI	CROATIA	FT-IR (B/P)
27	HR8	Hreljici	Quarry/outcrop	HGI	CROATIA	FT-IR (B/P)
28	HR9	Ljubici	Quarry/outcrop	HGI	CROATIA	FT-IR (B/P)
29	HR10	Marusici	Quarry/outcrop	HGI	CROATIA	FT-IR (B/P)
30	SLO7	MH	Quarry/outcrop	GEOZS	SLOVENIA	FT-IR (B/P)
31	SLO8	Kazlje	Quarry/outcrop	GEOZS	SLOVENIA	FT-IR (B/P)
32	SLO9	Gabrovica	Quarry/outcrop	GEOZS	SLOVENIA	FT-IR (B/P)

Legend:

MS= preparation of the cross section by embedding the sample in transparent epoxy resin
OM= analysis by optical microscope, with visible (VIS), ultraviolet (UV) or polarized light (POL)
FT-IR= analysis of the chemical composition by Fourier transform infrared spectroscopy
FT-IR (B/P), FT-IR (B), FT-IR (P) = FT-IR analysis of the patina (P) and/or the bulk (B) of the sample.
µFT-IR= micro FT-IR analysis by IR microscope
SEM= analysis of the surface by scanning electron microscope
SEM/EDS= microanalysis of the chemical composition by energy dispersive X-ray spectroscopy

SAMPLE LIST / Mechanical analysis						
Ord. n.	Sample ID	Object	Description/ position	Partner/ External ex.	Country	Analysis implemented
33	3107_S4	Debelo brdo - Benkovac	Outcrop	HGI	CROATIA	Flexural strength
34	3109_S3	3120 Benkovac PL-Benkovac (M-P)	Outcrop	HGI	CROATIA	Flexural strength
35	3303_S1	3320 Vinišće (M-Bi)	Outcrop+use	HGI	CROATIA	Flexural strength
36	3308_S1	3310 Milna-PL (G-R biokl.)	Outcrop	HGI	CROATIA	Flexural strength
37	3308_S2	3310 Milna-PL (Bi)	Outcrop	HGI	CROATIA	Flexural strength
38	3313_S1	Prapratnica (P kalc. Lam.)	Outcrop	HGI	CROATIA	Flexural strength
39	3314_S1	3330 Jelinak (P kalc.)	Outcrop	HGI	CROATIA	Flexural strength
40	3502_S1	Milna - M. Stiniva (M)	Outcrop	HGI	CROATIA	Flexural strength
41	3504_S1	3520 Vrboska PL (Bi)	Outcrop	HGI	CROATIA	Flexural strength
42	3505_S1	3520 Vrboska PL (Bi)	Outcrop	HGI	CROATIA	Flexural strength
43	3506_S1	3520 Vrboska PL	Outcrop	HGI	CROATIA	Flexural strength
44	3612_S1	3630 Gornji Humac-PL (P)	Outcrop	HGI	CROATIA	Flexural strength
45	3612_S2	3630 Gornji Humac-PL (P)	Outcrop	HGI	CROATIA	Flexural strength
46	3612_S3	3630 Gornji Humac-PL (P)	Outcrop	HGI	CROATIA	Flexural strength
47	3702_S1	Gornji Humac PL - Vis (P)	Outcrop	HGI	CROATIA	Flexural strength
48	3807_S1	Milna-PL (Vela Luka, M/W/P)	Outcrop	HGI	CROATIA	Flexural strength
49	3813_S1	3820 Milna-PL (Žrnovo, P)	Outcrop	HGI	CROATIA	Flexural strength
50	3813_S3	3820 Milna-PL (Žrnovo, P)	Outcrop	HGI	CROATIA	Flexural strength
51	3905_S1	3910 Gornji Humac PL (P/M)	Outcrop	HGI	CROATIA	Flexural strength
52	3917_S1	Milna PL - Nakovana (Bi)	Outcrop	HGI	CROATIA	Flexural strength
53	3918_S1	Milna PL – Nakovana (M)	Outcrop	HGI	CROATIA	Flexural strength
54	SLO7	Gabrovica	Outcrop	GEOZS	SLOVENIA	Flexural strength
55	SLO8	Griza	Outcrop	GEOZS	SLOVENIA	Flexural strength
56	SLO9	MH	Outcrop	GEOZS	SLOVENIA	Flexural strength
57	SLO10	Gabrovica	Outcrop	GEOZS	SLOVENIA	Compressive strength
58	SLO11	Griza	Outcrop	GEOZS	SLOVENIA	Compressive strength
59	SLO12	Kazlje	Outcrop	GEOZS	SLOVENIA	Compressive strength
60	SLO13	Mh	Outcrop	GEOZS	SLOVENIA	Compressive strength

61	ZAD 2	Austro-hungarian sidewalk- Zadar	Sidewalk	Silvije Pranjić (ZADRA NOVA)	CROATIA	Porosity
62	ZAD 3	Medviđa, sv. Ivan Krstitelj	Roof of the church	Silvije Pranjić (ZADRA NOVA)	CROATIA	Porosity
63	SLO1	Škrateljinova domačija, Divača	Roof	ZRS Koper	SLOVENIA	Porosity
64	SLO2	Pri Blaževih	Roof	ZRS Koper	SLOVENIA	Porosity
65	SLO4	Cerkev Marijinega vnebovzetja -Šmarje pri sežani	Roof	ZRS Koper	SLOVENIA	Porosity
66	ITA 1	Trebiciano 107	Roof	diGEO- UNITS	ITALY	Porosity
67	n. 1104	Rupinpiccolo 17	Roof	diGEO- UNITS	ITALY	Porosity
68	HR2	Zrenj 1 ZR1	Quarry/outcrop	HGI	CROATIA	Porosity
69	HR3	Zrenj 2 ZR2	Quarry/outcrop	HGI	CROATIA	Porosity
70	HR7	Laganisi	Quarry/outcrop	HGI	CROATIA	Porosity
71	SLO14	Gabrovica	Quarry/outcrop	GEOZS	SLOVENIA	Porosity

Preliminary microscopic observations

In order to determine the analysis, each sample was preliminarily observed and described with the aid of a stereomicroscope. It was determined which parts (patina, bulk, surface impurities) has to be analyzed, and which method to apply for their analysis. Each sample was photographed by the magnification of 6 to 30X.

Sample: ID 3400 Grohote – Ruića Dvora - roof (HGI) – Mag. 10X

There are visible some beige-yellowish patinas on the surface of the sample. Degradation by layering is visible and changes in colour of the stone.

Sample: ZAD 3 Medviđa sv. Ivan Krstitelj – Roof - Mag. 20X.

The biological deterioration concerns only the surface of the sample where are visible endolithic lichens colonies.

Sample: ZAD 4 Medviđa sv. Ivan Krstitelj – Presbytery - Mag. 10X.

Grey patina and endolithic lichens visible on the surface.

Sample: ZAD 5 Medviđa sv. Ivan Krstitelj – Sidewalk - Mag. 20X.

Structural deterioration is visible on the surface and the bulk of the sample. Endolithic lichens are present too.

Sample: ZAD 6 Ovča quarry Dugi otok - Mag. 20X.

On the exposed, left, part of the sample, a grayish patina is visible. Holes caused by endolithic lichens are present.

Sample: Slo1 Škrateljinova domačija – Roof – mag. 10X

Degradation by layering and disintegration of material is visible as well as lichens and impurities on the stone surface.

Sample: Slo2 Pri Blaževih – Roof – mag. 10X

Lichens of various typology are visible on the sample surface.

Sample: Slo3 Cerkev Marijinega vnebovzetja na Guri – Roof – mag. 10X

Lichens of various typology are visible on the sample surface

Sample: Slo4 Cerkev Marijinega vnebovzetja – Roof – mag. 10X	
	
Lichens of various typology are visible on the sample surface. The bulk of the sample has a darker coloration than the surface.	

Sample: Slo5 Cerkev Marijinega vnebovzetja – Wall below the presbytery – mag. 10X

It is a sample of mortar. Aggregates and the binder matrix are recognizable.

Sample: Slo6 Cerkev sv. Elije – Foundation – mag. 10 and 20X

Significant degradation due to exfoliation and layering is visible. The bulk of the sample has a darker coloration than the surface patina, which may have been altered and decolorized by weathering agents.

Sample: Ita1 Trebiciano 107 – Roof – mag. 10X

Degradation due to exfoliation and layering is visible as well as lichens on the stone surface.

Sample: Ita2 Rupingrande 31 – Roof – mag. 10X

No significant degradations are visible, a greyish thin patina is observable on the exposed side of the sample.

Sample: n1039 Basovizza- Kosovel 28 – Roof – mag. 10X

A thick lichen colony is present on the stone surface of the studied sample.

Sample: n1100 Rupinpiccolo 4 – Roof – mag. 10X

No significant degradation are observable on the sample surface. Micro fractures are visible as well as layering of the stone structure.

Sample: n1104 Rupinpiccolo 17 – Roof – mag. 10X

A yellowish-beige patina is observable on the sample surface. No biological degradation are present.

Cross-sections preparation, optical microscopy, scanning electron microscopy and microanalysis (SEM/EDS) and infrared spectroscopy (FT-IR, µFT-IR)

Several samples were embedded in transparent epoxy resin, polished an observed by optical microscope applying different microscopic techniques (VIS, Polarized, UV light). This method allows the analysis of the surface patina on the sample, the determination of the type of degradation and estimation of its extent to the bulk of the sample rock. Afterwards, samples which presented considerable degradations, were analyzed by scanning electron microscope (SEM/EDS) in order to study the degradation in detail and to determine the chemical composition of the altered stone structure. Finally, with the purpose of a complete chemical definition of all the individuated degradation typologies, individual layers were analyzed using micro-infrared spectroscopy (µFT-IR) which allows molecules' structure characterization.

Sample: ID 3400 Grohote – Ruića Dvora – cross-section – Mag. 10X

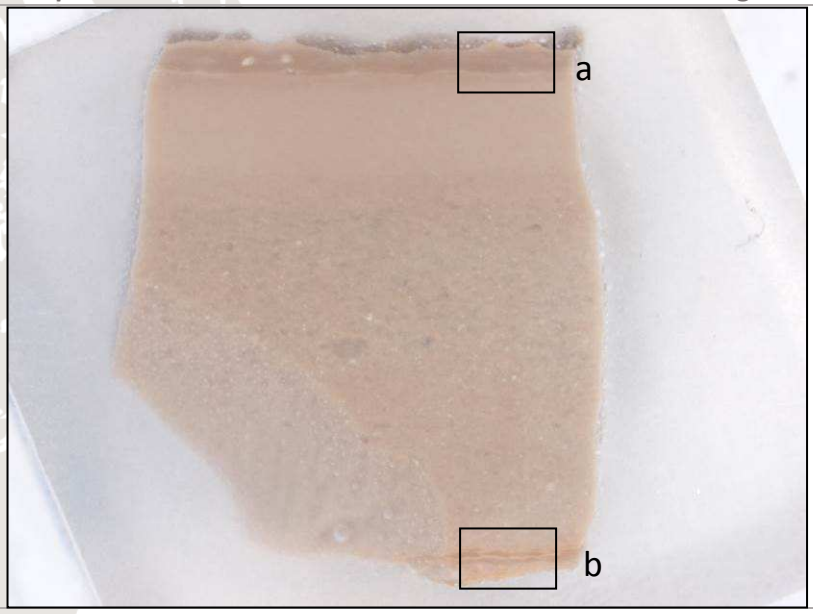

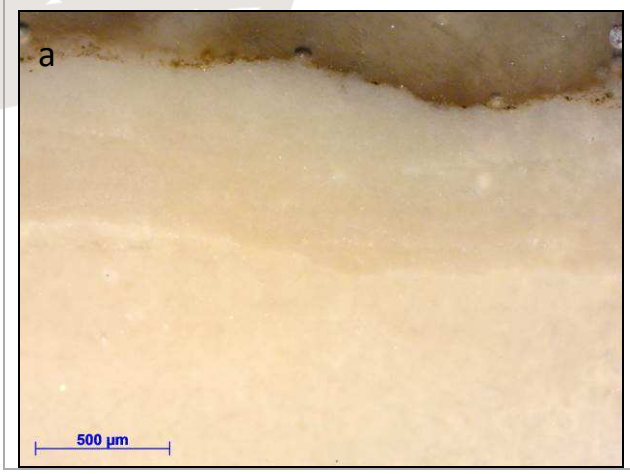

On the sample there is visible a layered structure. The two exposed surfaces of the sample both present some alterations, which manifest themselves in the stratification of the surface structure of the stone in the first 500 microns of the sample bulk.
The surface patina has no significant thickness, no considerable biodegradation or crusts are observable.

Sample: ZAD 3 Medviđa sv. Ivan Krstitelj – Roof – cross-section Mag. 12X.

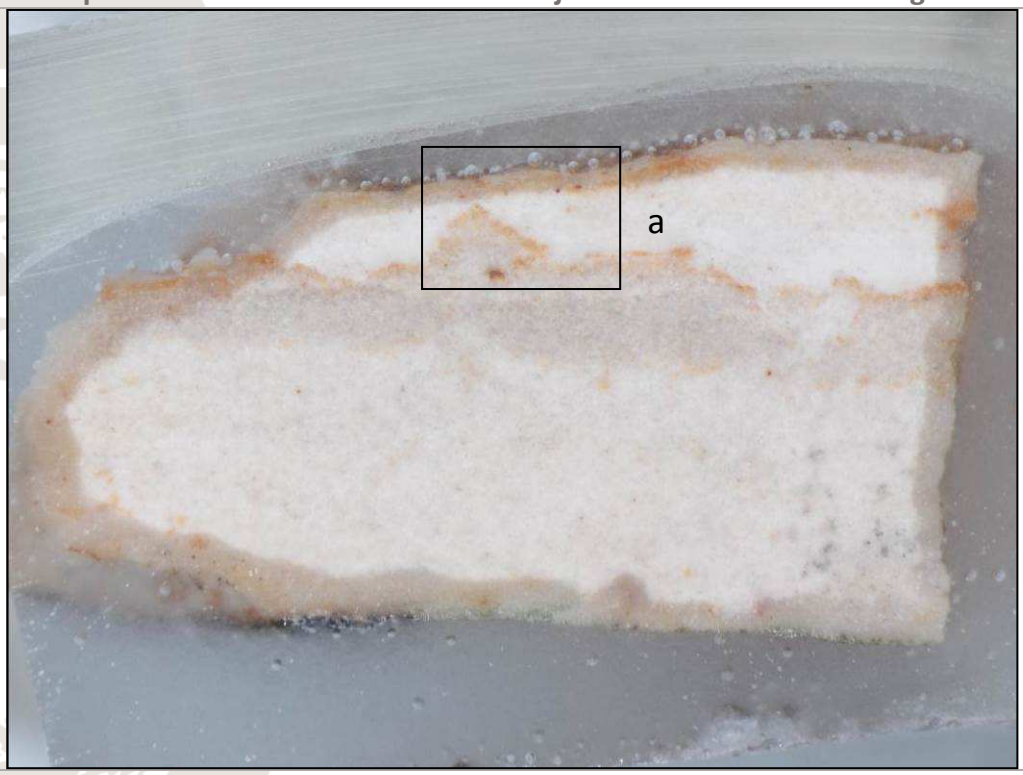

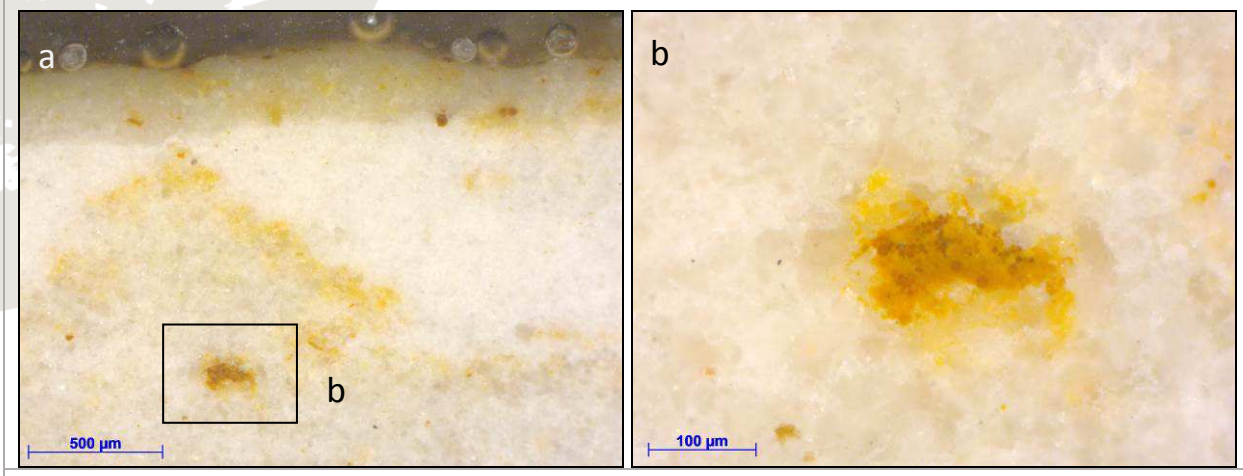

Absorption of the transparent epoxy resin by the first 100 to 500 micrometers of the stone structure is visible, which imply that the porosity of the analyzed sample is relatively low. Layers with different colors and alterations in the structure are observable along the sample cross-section. Alterations in color due to the presence of iron oxide crystals are visible as orange stains.

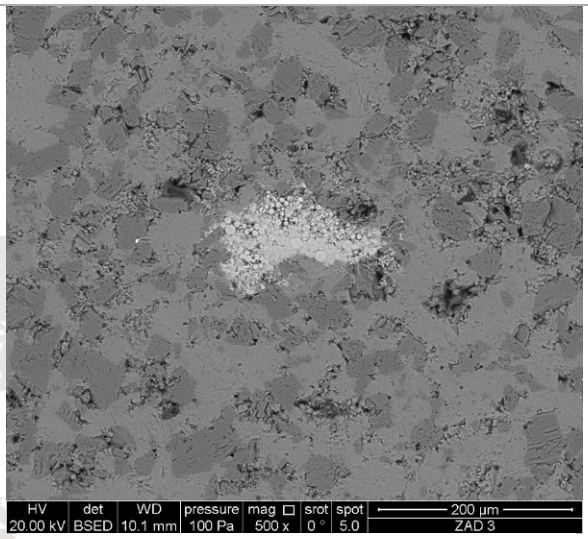

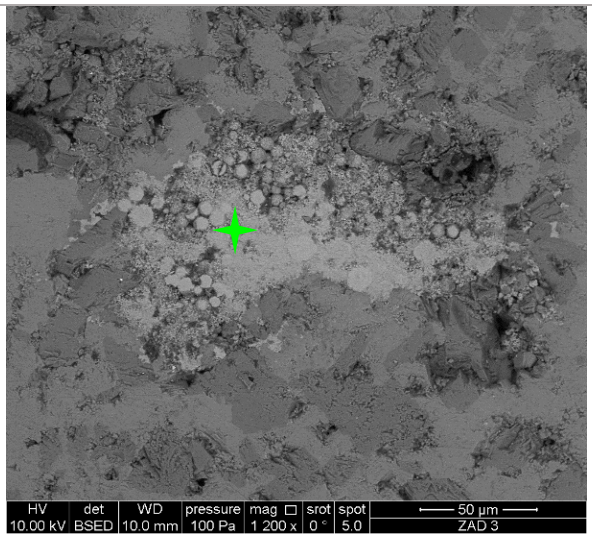

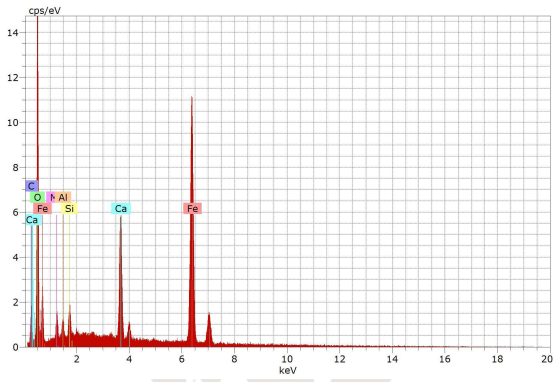

Spectrum: Acquisition

El	AN	Series	unn. C [wt.%]	norm. C [wt.%]	Atom. C [at.%]	Error (1 Sigma) [wt.%]
Fe	26	K-series	43.56	42.01	17.94	1.22
O	8	K-series	40.42	38.98	58.10	5.50
C	6	K-series	8.68	8.38	16.63	1.85
Ca	20	K-series	7.85	7.57	4.50	0.27
Mg	12	K-series	1.52	1.47	1.44	0.13
Si	14	K-series	0.95	0.91	0.77	0.08
Al	13	K-series	0.72	0.70	0.61	0.07
Total:			103.70	100.00	100.00	

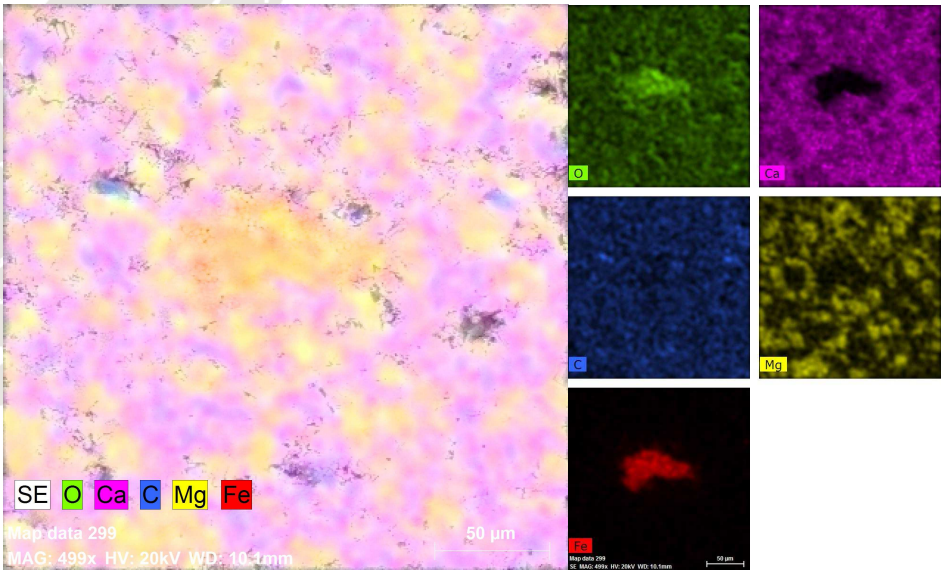

SEM/EDS analyses confirmed the presence of iron oxide. Furthermore BSE image and EDS maps show the presence of magnesium (coloured in yellow) in the stone structure indicating that the sample is a dolomitic limestone.

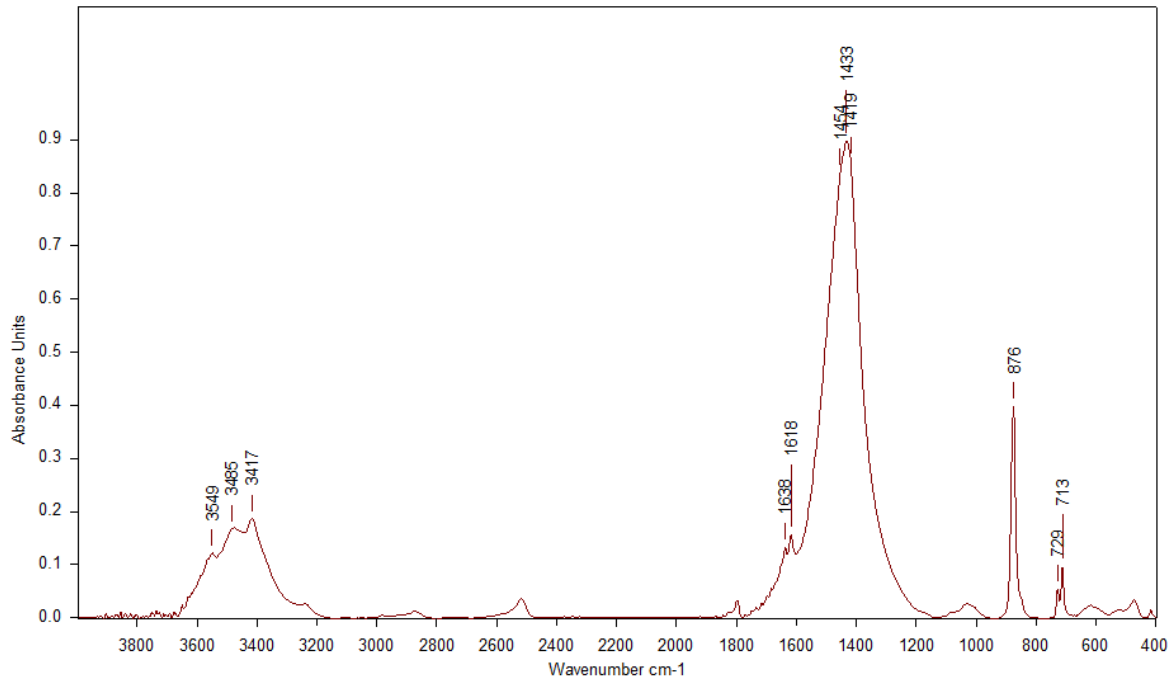

FT-IR spectra of the sample ZAD 3 shows typical calcite bands: at 1433 cm^{-1} stretching of the C-O bonds in the carbonate ion is observable, while bands at 876 and 713 cm^{-1} correspond to the bending of CO_3^{2-} ion. The band at 729 cm^{-1} indicates the in-plane bending mode (v4) of CO_3^{2-} in the dolomite structure. Bands in the zone 3550 – 3415 cm^{-1} correspond to water molecules present as humidity.

Sample: ZAD 4 Medviđa sv. Ivan Krstitelj – Presbytery – cross-section Mag. 12X.

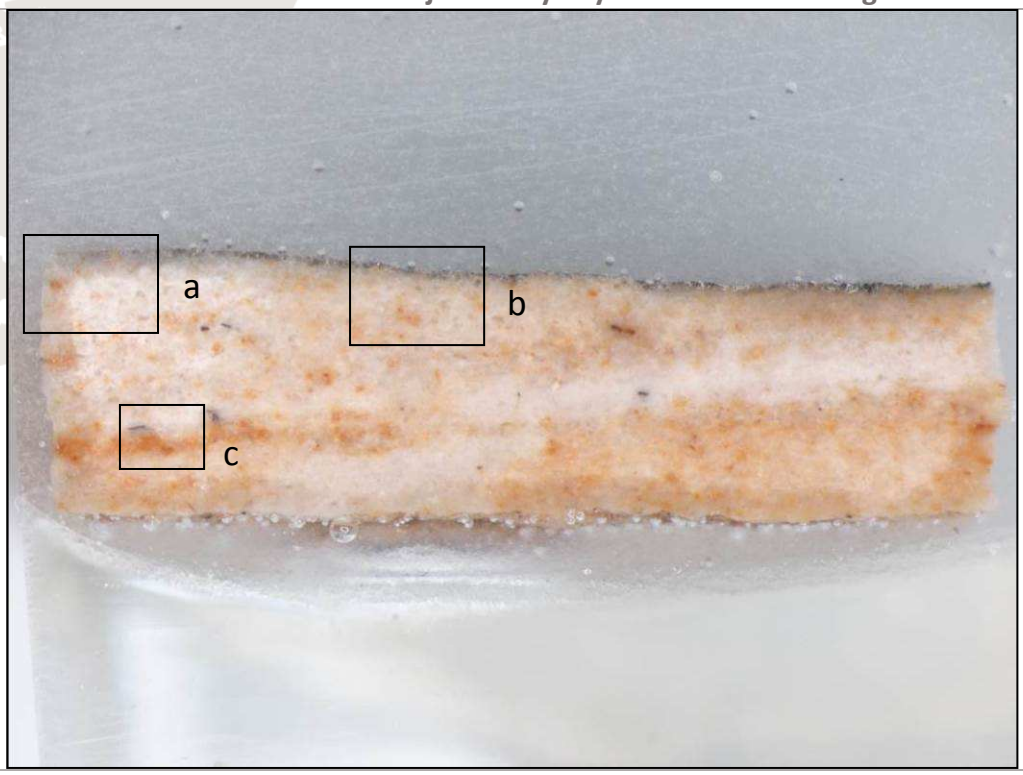

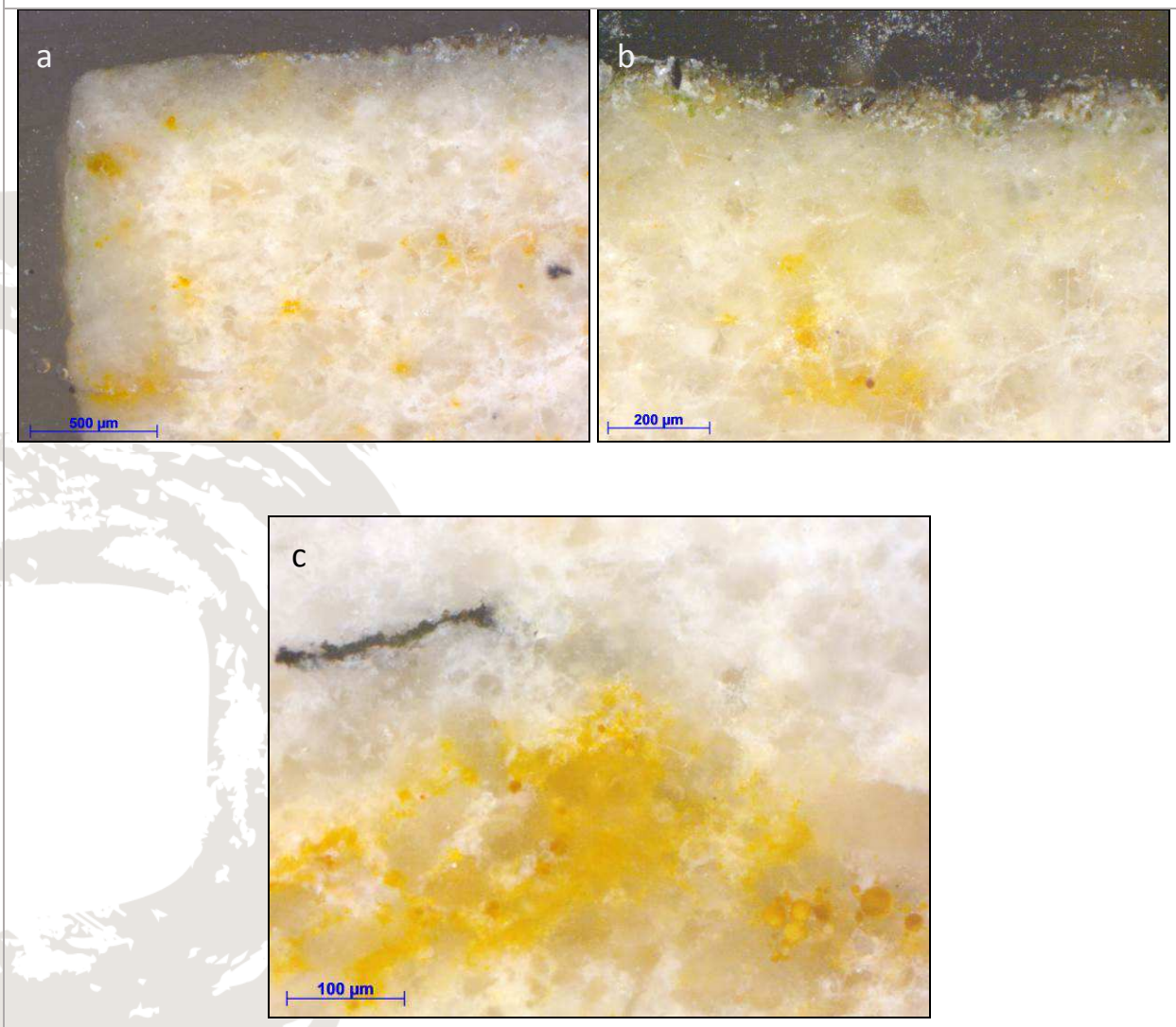

Absorption of the transparent epoxy resin by the first 100 to 500 micrometers of the stone structure is visible, which imply that the porosity of the sample is relatively low. Layers with different coloration are recognizable and numerous orange stains due to the presence of iron oxide are visible in form of spherical crystals (figure C).

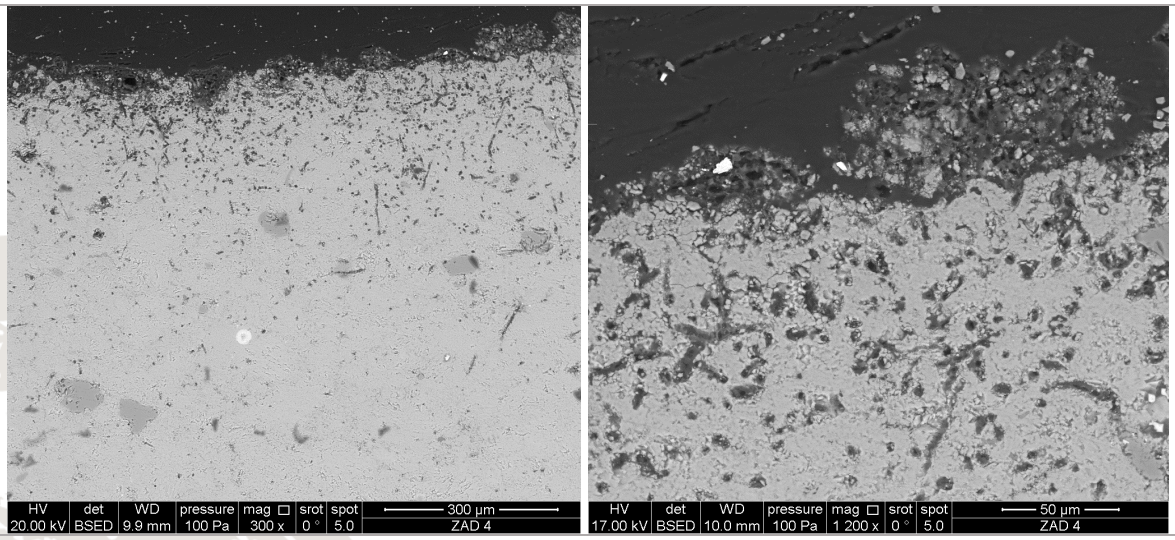

SEM BSE images show a dense layer of hyphae actively penetrating and dissolving the calcite structure.

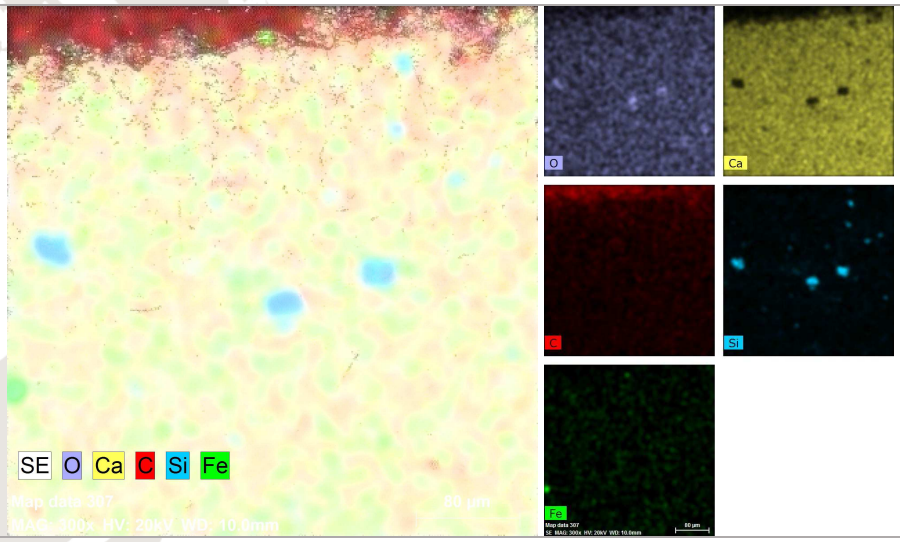

EDS map shows no change in composition on the stone surface, just a lowering in the calcium concentration has been registered. Single element maps illustrate the presence of silicon oxide particles, as well as iron oxide inclusions.

Sample: ZAD 5 Medviđa sv. Ivan Krstitelj – Sidewalk - Mag. 20X

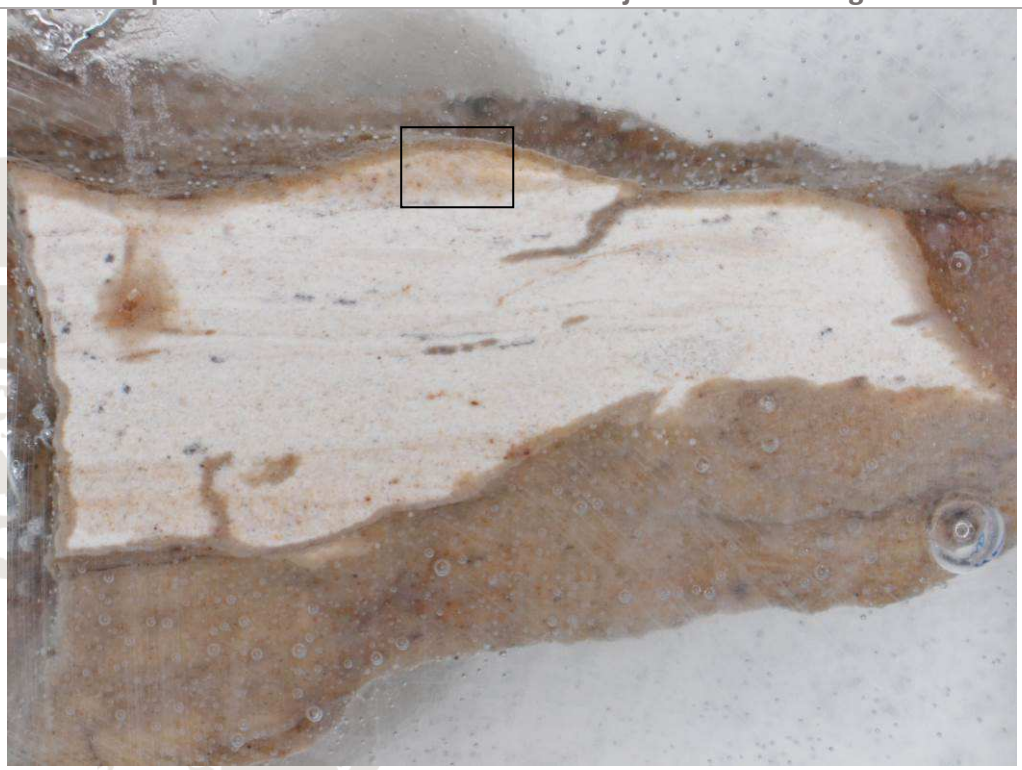

As in the two previous samples, absorption of the transparent epoxy resin in the first 500 micrometers of the stone structure is visible, as well as in the micro-fracture observable in the sample.

Sample: Slo1 Škrateljinova domačija – Roof – mag. 10X

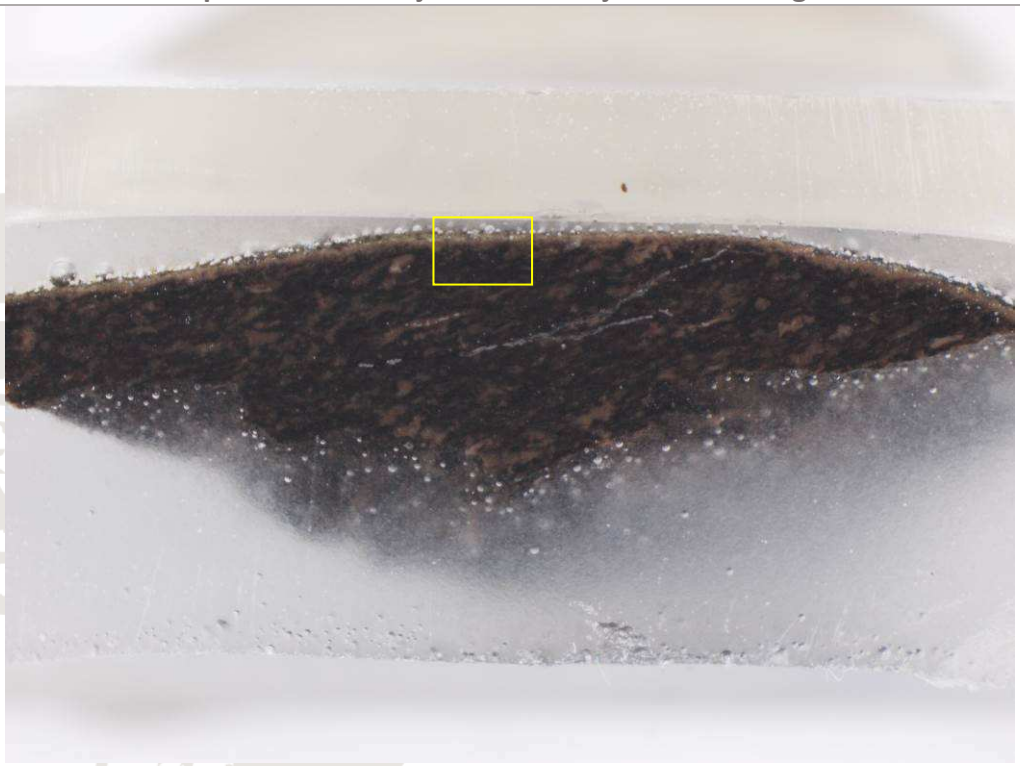

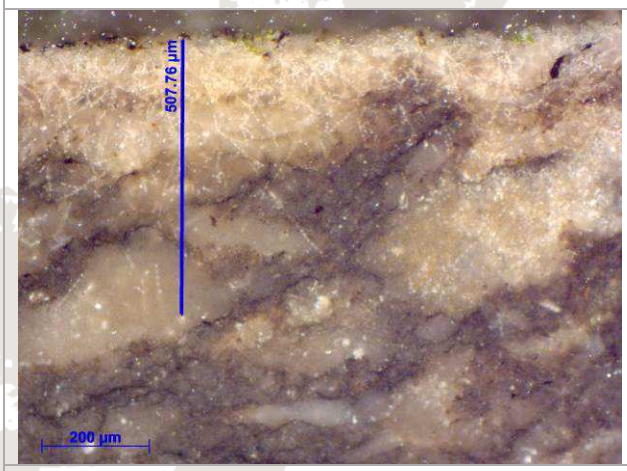

On the sample it is visible a slightly discoloration of the rock on the surface due to hyphae of endolithic lichens present on the rock surface. The colonization of the studied sample goes up to half millimeter in the rock structure increasing the porosity and damaging the carbonate crystal structure in the affected area. On the surface of the studied sample no noteworthy patina is observable.

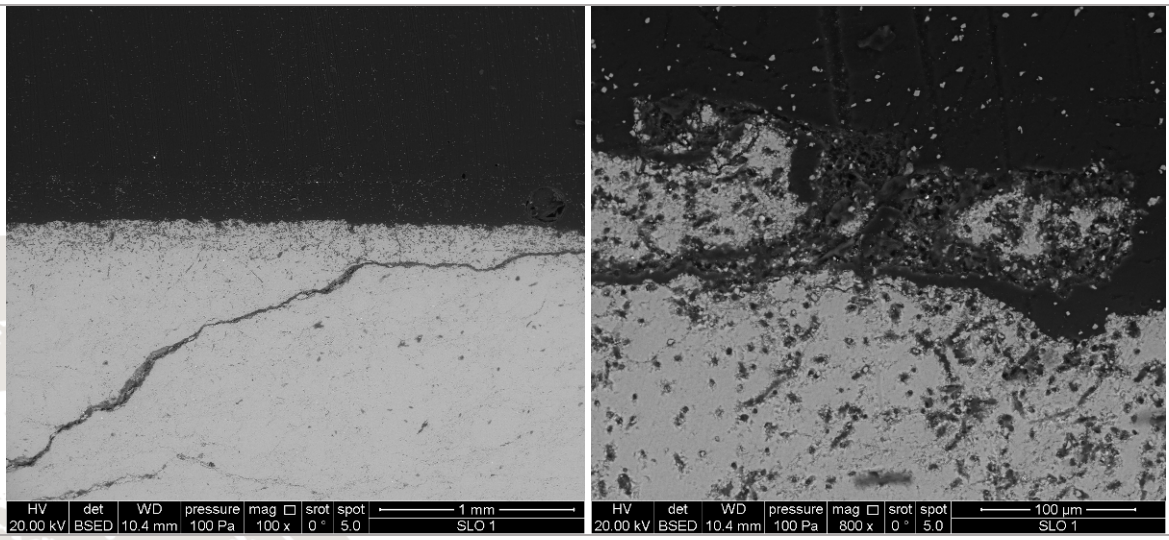

SEM BSE images point out fractures along the analyzed sample and on its exposed surface where damage and detachment of material can be observed due to the activity of endolithic lichens.

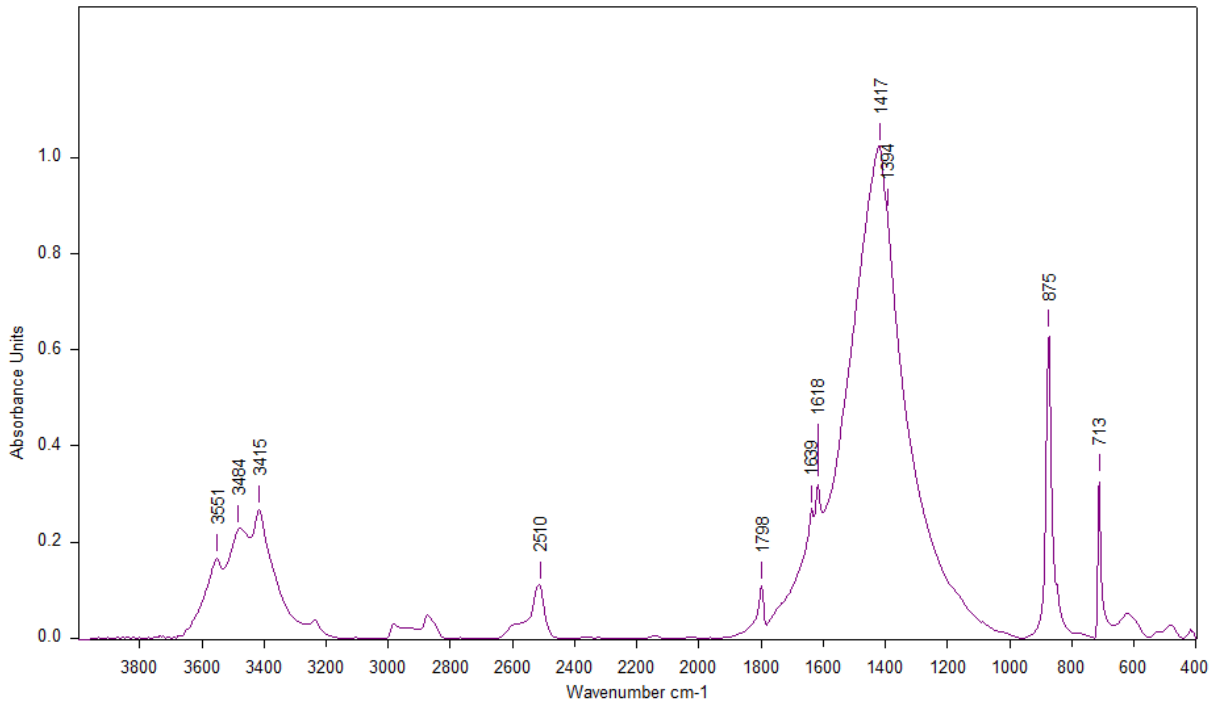

FT-IR spectra of Slo1 sample shows calcite bands at 1417 cm^{-1} stretching of the C-O bonds in the carbonate ion is present, bands at 876 and 713 cm^{-1} correspond to the bending of CO_3^{2-} ion. Bands in the zone 3550 – 3415 cm^{-1} correspond to water molecules present as humidity.

Sample: Slo2 Pri Blaževih – Roof – mag. 10X

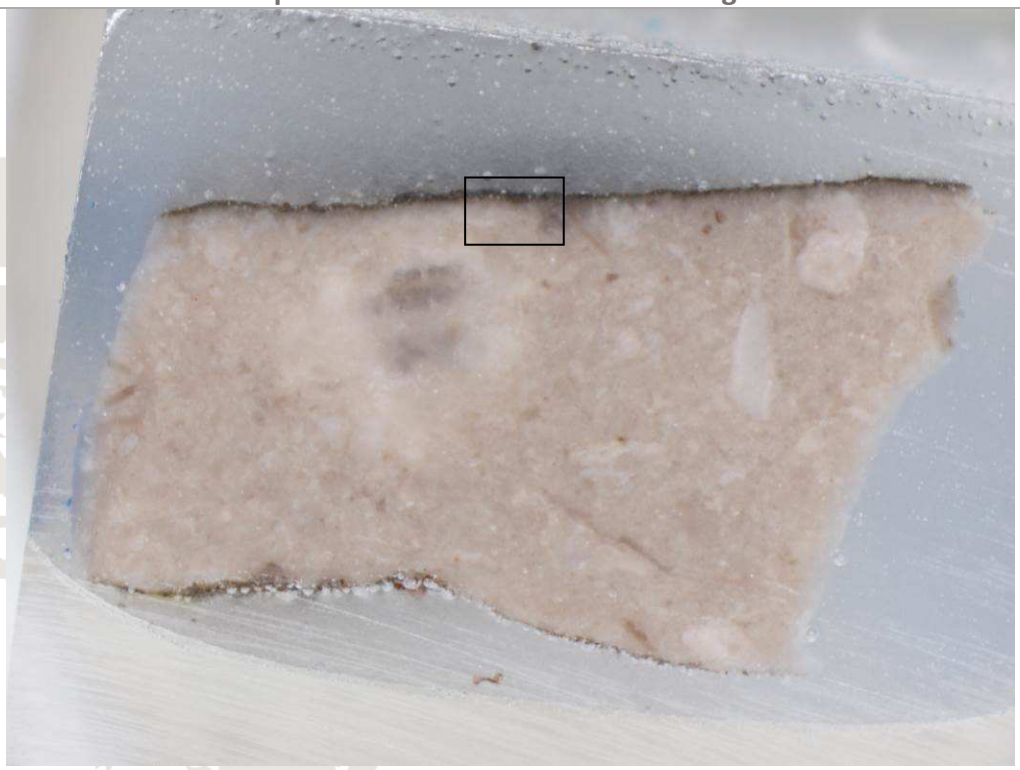

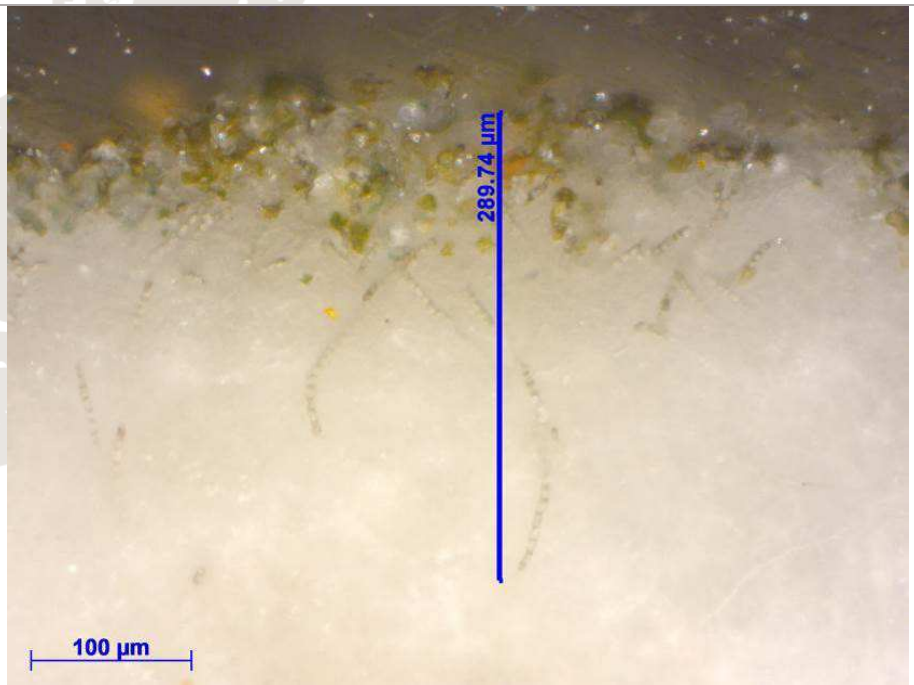

A thin greyish patina is visible on the sample surface. A more detailed microscopic analysis showed its biological origin. The lichens hyphae penetrated the stone bulk up to 300 micrometers. On the studied sample no layering is visible.

Sample: Slo4 Cerkev Marijinega vnebovzetja – Roof – mag. 12X

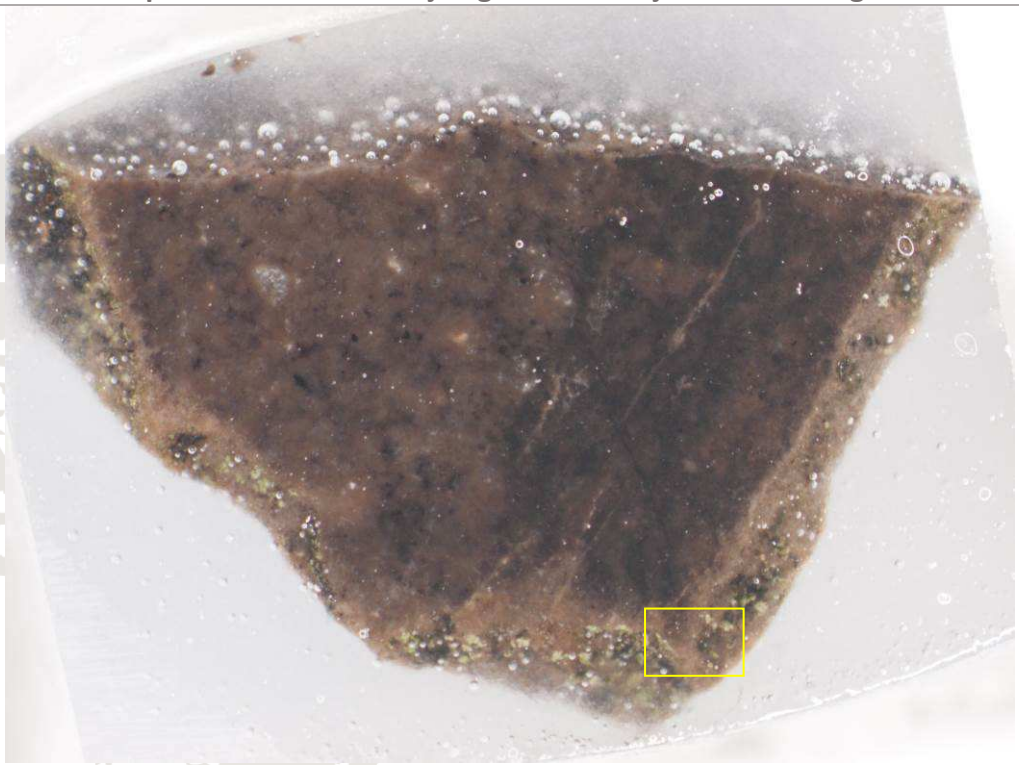

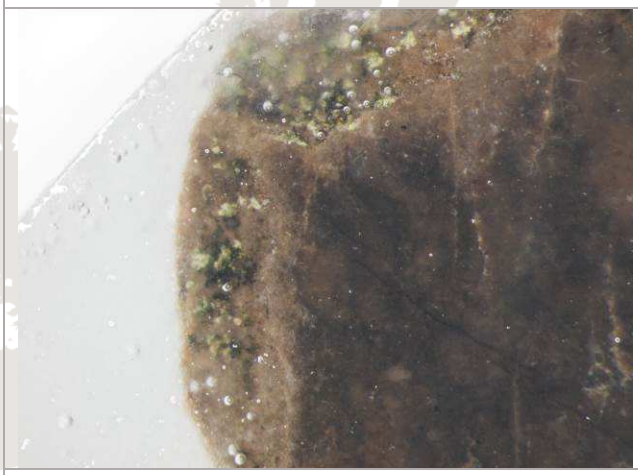

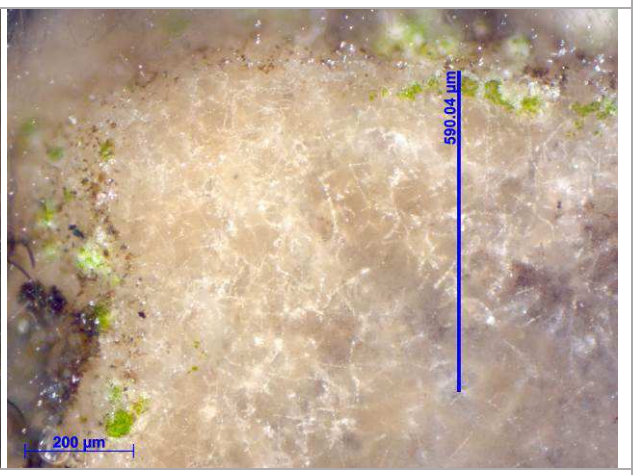

On the studied sample a slightly discoloration of the rock on the surface has been noticed, due to hyphae of endolithic lichens present on the rock surface. The colonization of the studied sample goes up to more than half millimeter in the rock structure increasing the porosity and damaging the carbonate structure.

Sample: Slo5 Cerkev Marijinega vnebovzetja – Wall below the presbytery – mag. 12X

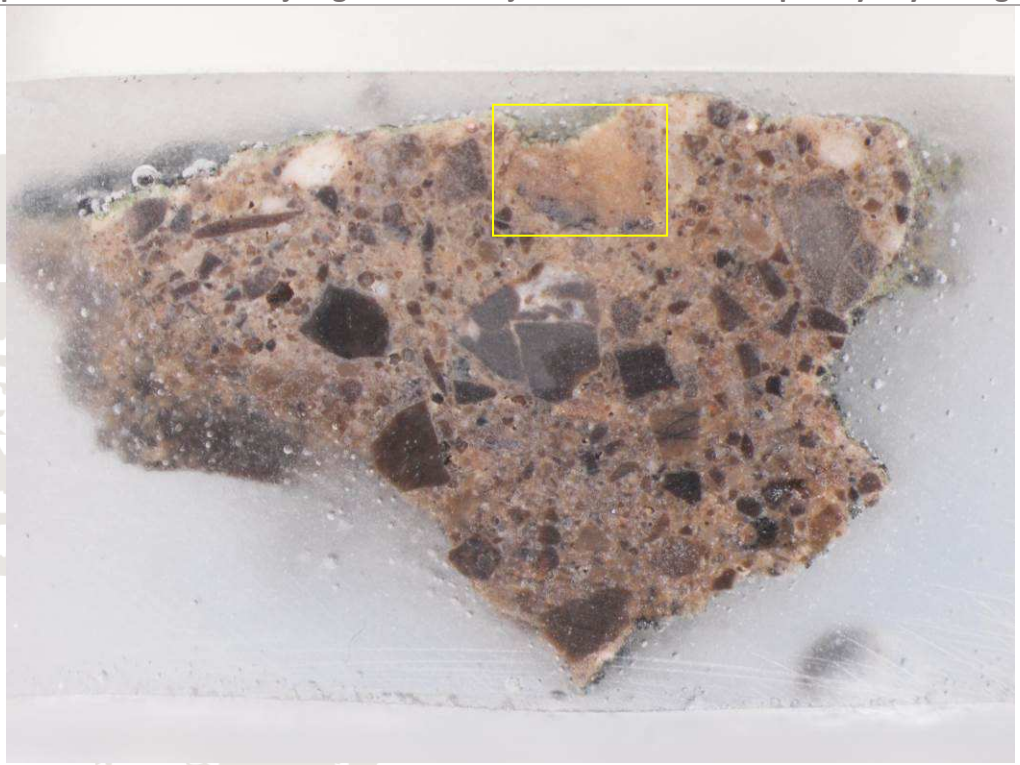

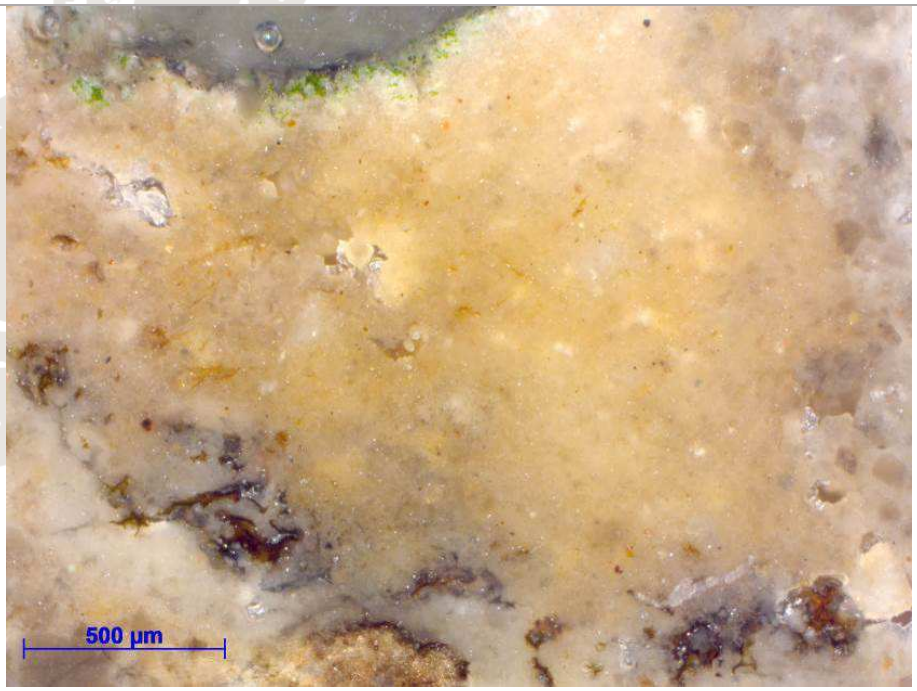

The sample studied is a mortar where aggregates and the binder matrix are visible. The aggregates are mostly crushed limestone greyish color. The aggregates/binder ratio is about 50%. On the exposed surface of the sample a green layer is visible due to the presence of lichens.

Sample: Slo6 Cerkev sv. Elije – Foundation – mag. 20X

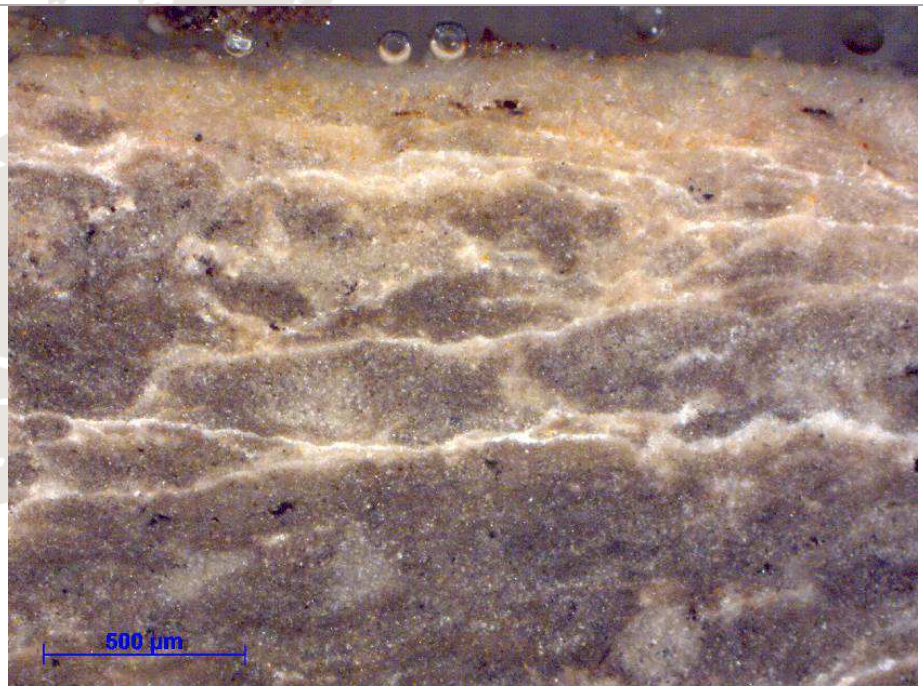

Significant stratification of the lithotype is visible in the studied sample as well as superficial discoloration although any patina of biological origin is present. Orange colored crystals are visible along the first 1000 micrometers of the sample cross-section.

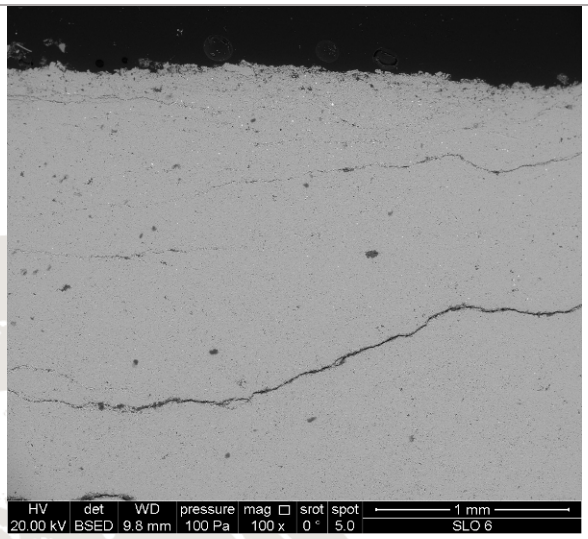

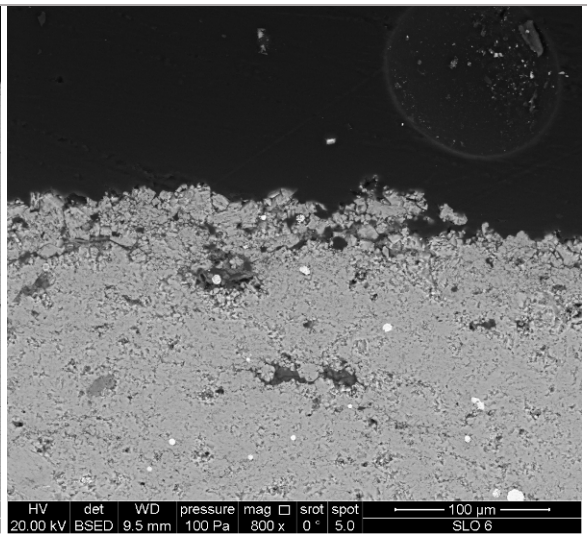

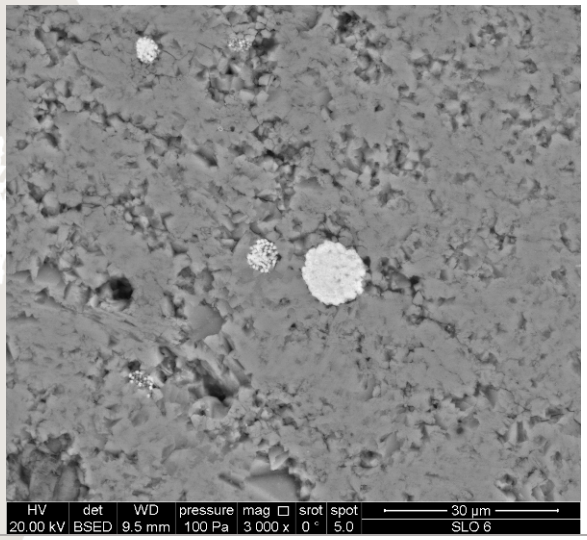

SEM BSE images show layering in the stone structure and significant loss of cohesion in the superficial part of the surface. Spherical crystals of iron oxide are visible along the analyzed sample surface.

Sample: Ita1 Trebiciano 107 – Roof – mag. 20X

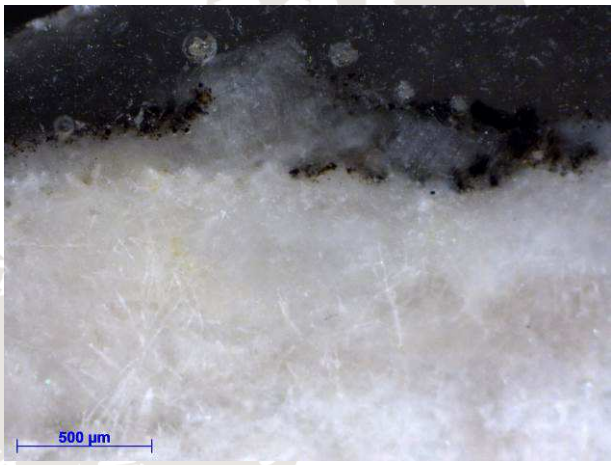

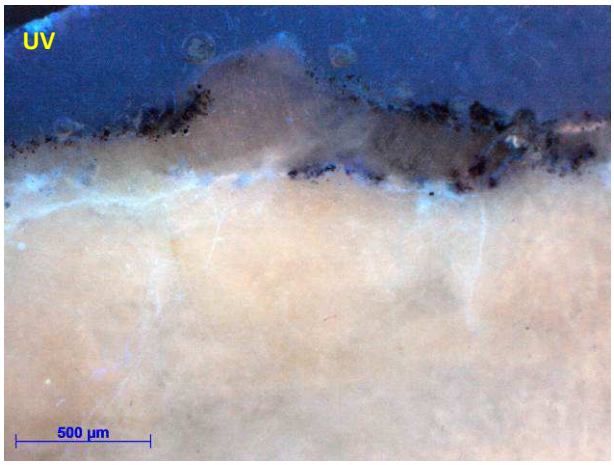

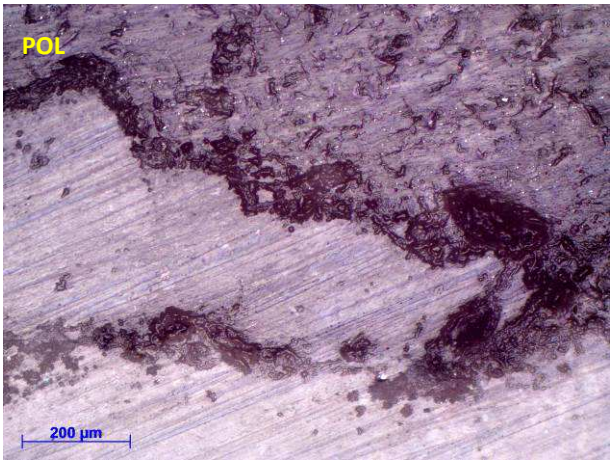

Damages in the structure are visible in the first millimeter beneath the exposed stone surface due to the presence of lichens whose growth caused fissure of limestone crystals. UV light points out the structure alterations and deposition of crystallized $CaCO_3$ in the fissures while with polarized light limits of the same zone are clearly highlighted.

Sample: Ita2 Rupingrande 31 – Roof – mag. 30X

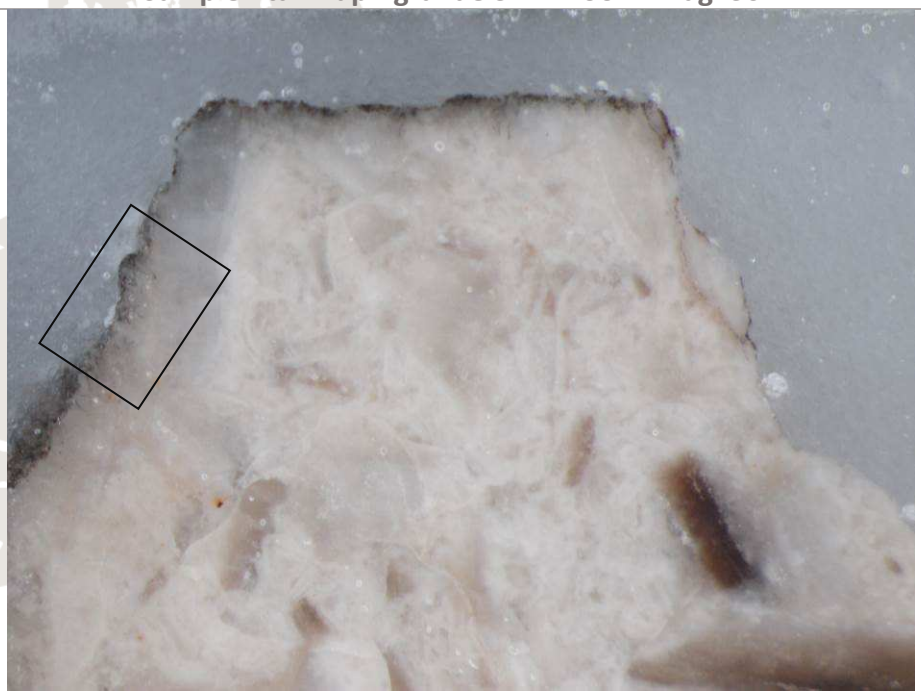

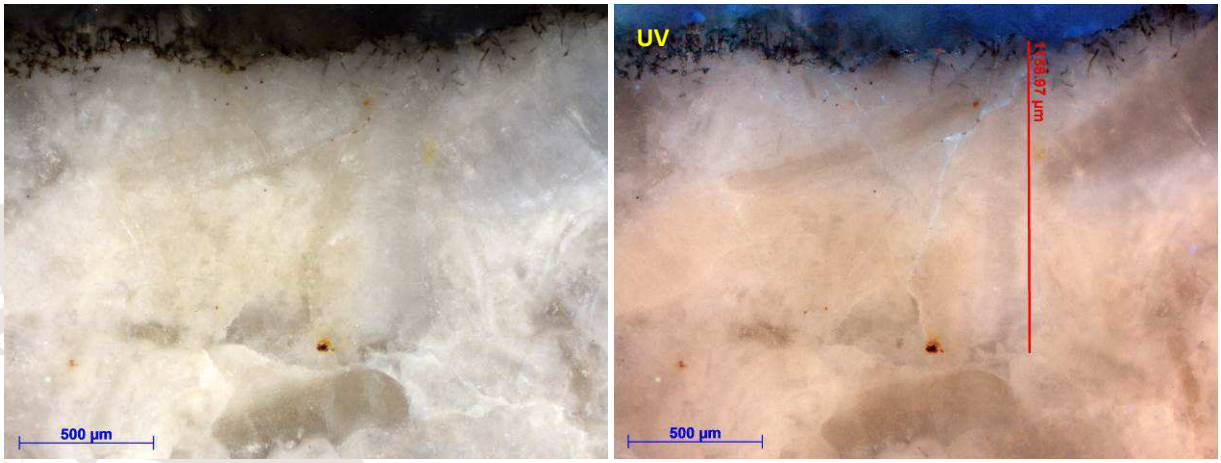

Fractures of the stone structure are visible up to 1 millimeter beneath the exposed surface of the analyzed sample. UV light points out the fractures, where recrystallized carbonate is probably present. Roots of lichen colonies are visible on the sample surface.

Sample: n.1039 Basovizza – Kosovel 28 – Roof – mag. 20X

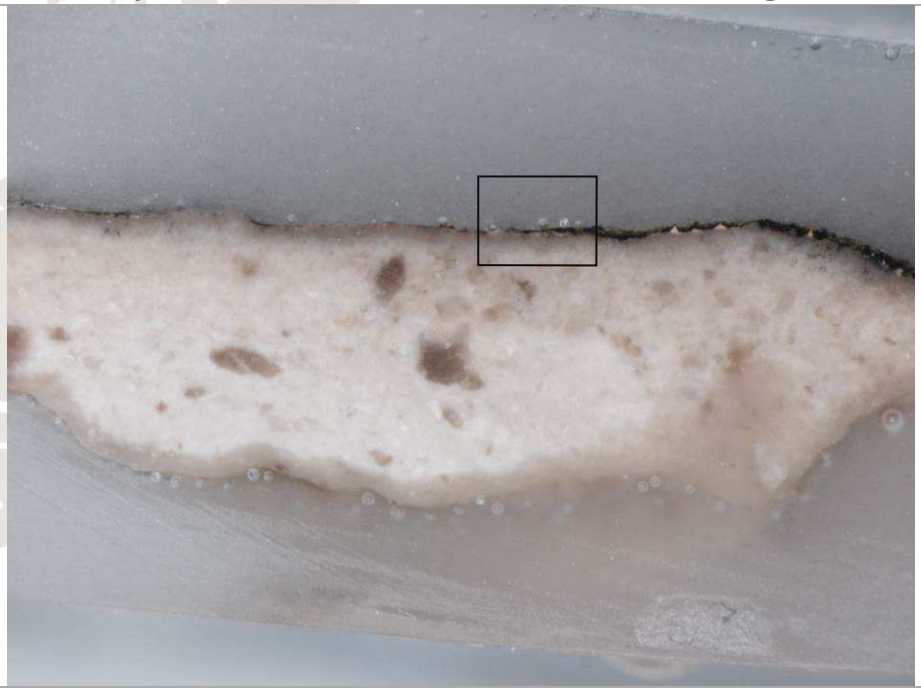

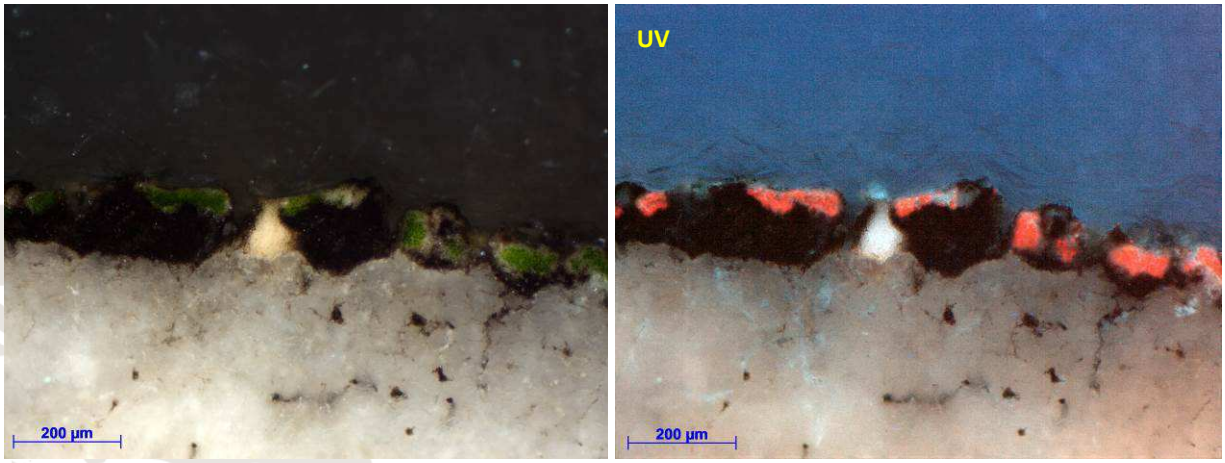

A thin dark patina is observable on the analyzed sample surface due to the presence of lichens. Strong red fluorescence of the lichen under UV light denotes it is still active and has optimal photosynthetic capacity.

Sample: n.1100 Rupinpiccolo 4 – Roof – mag. 20X

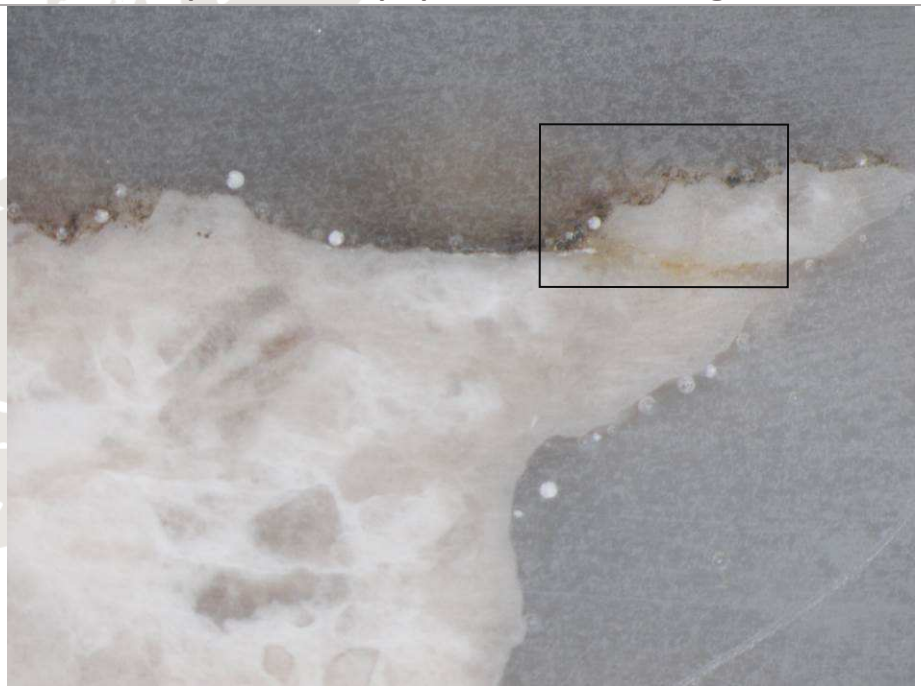

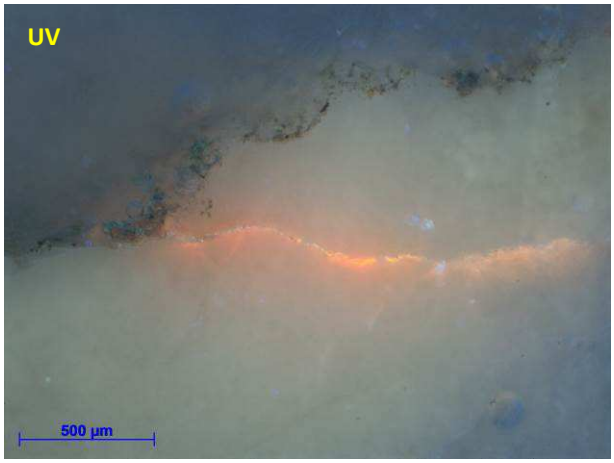

Lichens colonies are present on the stone surface as well as fissures are visible. Strong orange absorption in the crack due to infiltrations of solubilized and recrystallized $CaCO_3$.

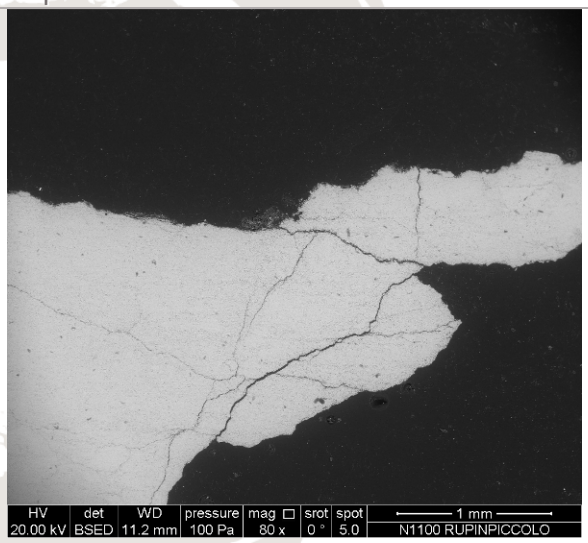

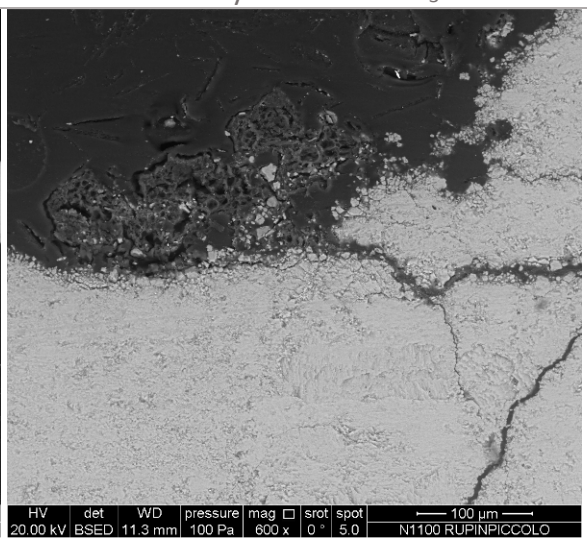

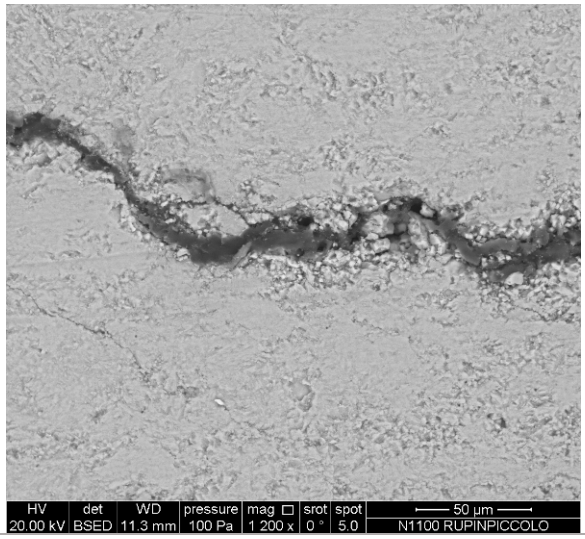

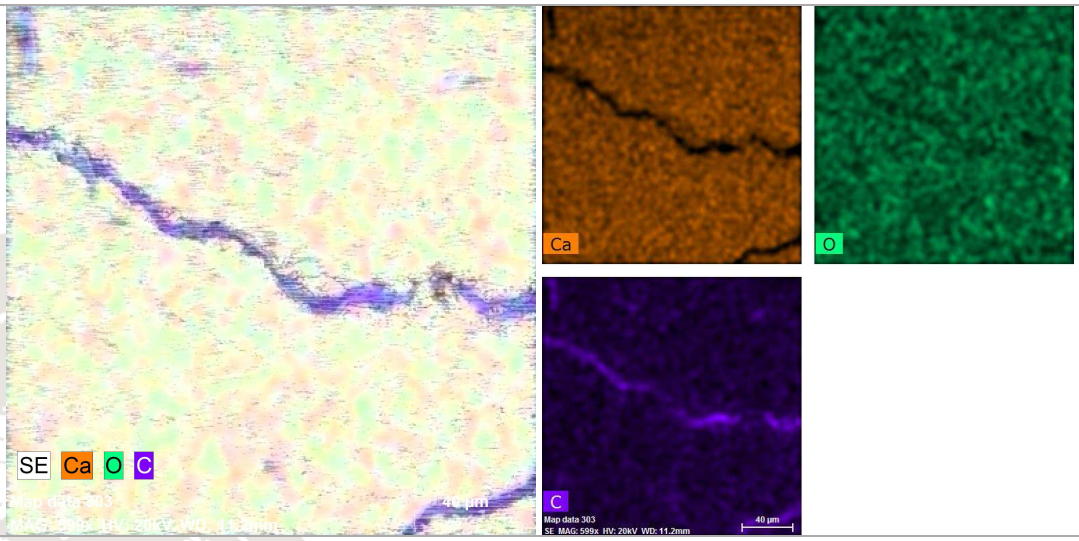

SEM/EDS analyses show no changes in composition in the observed fissure. The higher concentration of carbon presented in elemental maps, is due to the infiltration of the embedding resin. These results confirm the assumption of solubilized and recrystallized carbonate deposited in the fissure.

Sample: n.1104 Rupinpiccolo 17 – Roof – mag. 20X

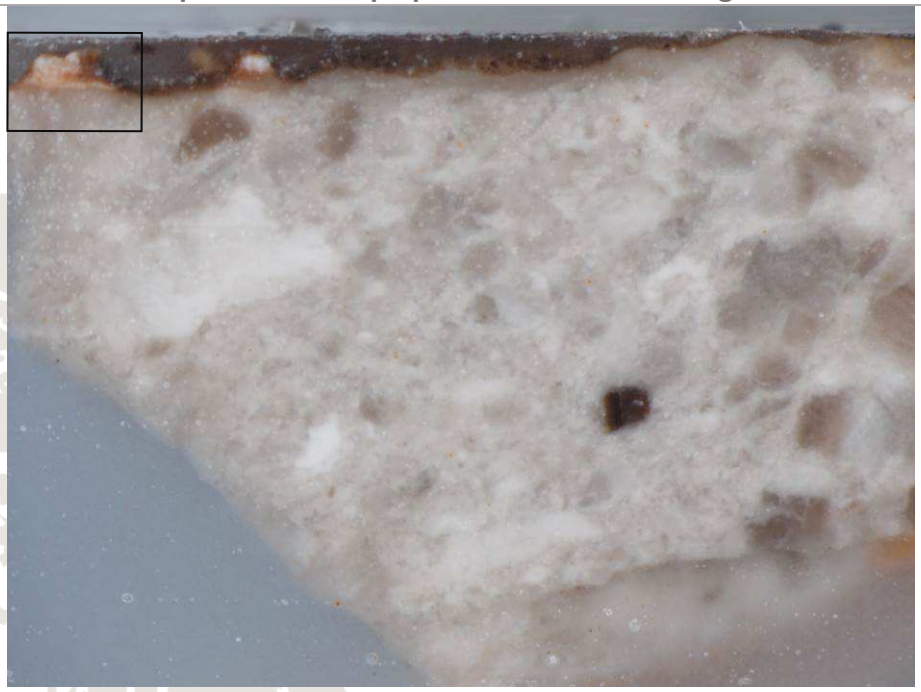

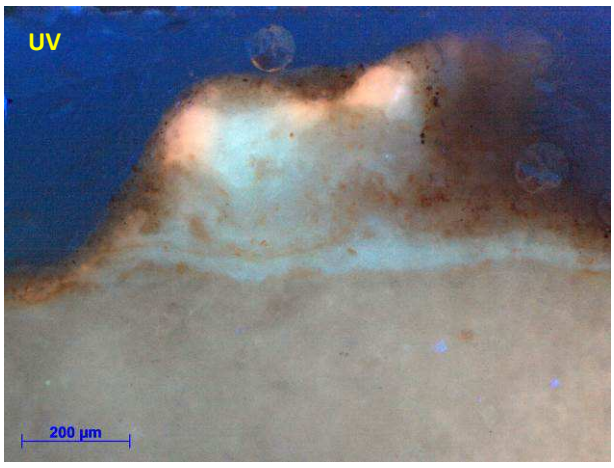

A beige patina is observable on the sample surface. Microscopic analysis point out different UV absorption in several zone on the surface due to the different structure of the recrystallized carbonate on the sample surface.

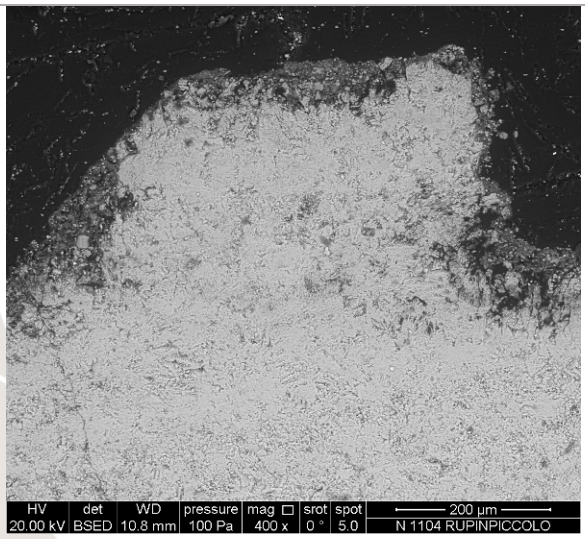

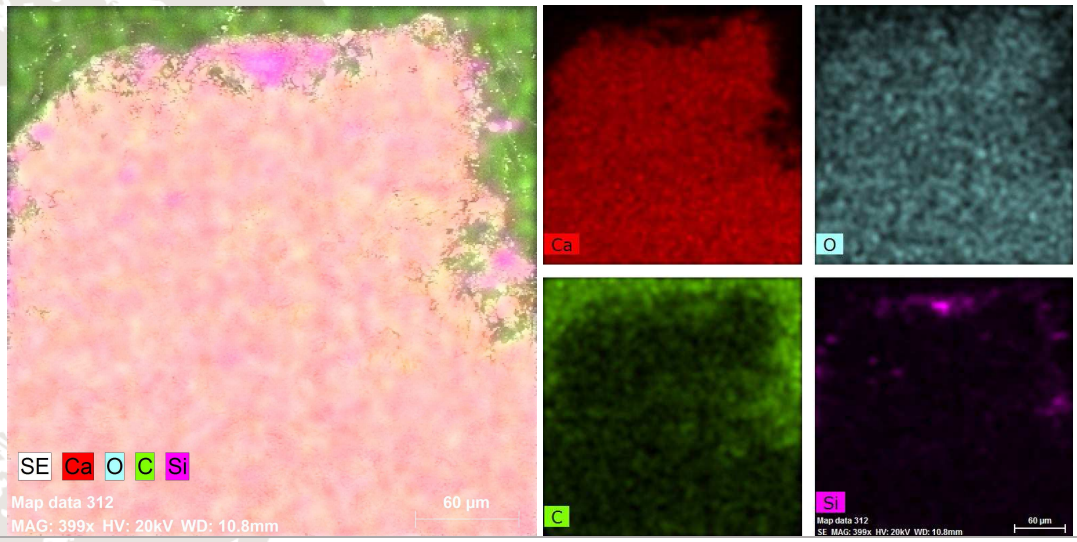

SEM/EDS analyses show no changes in the carbonate composition or structure on the sample surface, confirming the UV absorption by recrystallized calcium carbonate.

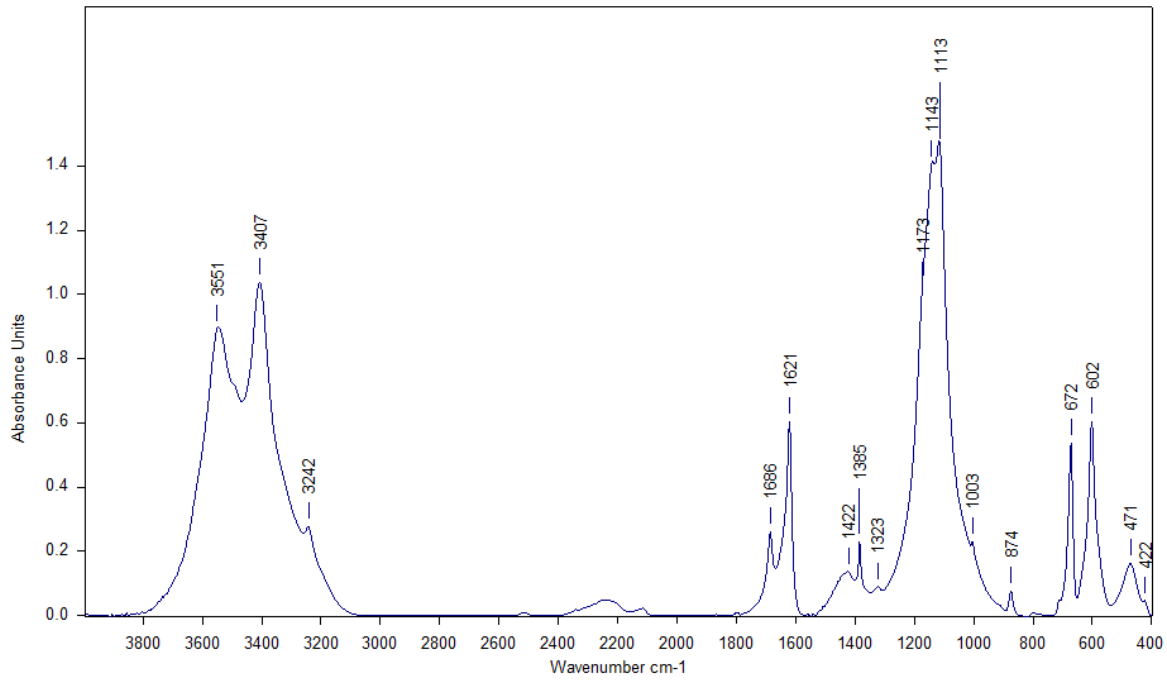

By means of SEM/EDS a portion of sample without sulfur was analyzed, for FT-IR analysis from another part of the sample, some superficial patina was taken and the spectrum obtained shows the it was made mainly of calcium sulphate dihydrate (gypsum). Peaks at 1143 cm^{-1} and 1113 cm^{-1} indicate asymmetric SO_4^{-2} stretching band while at 672 cm^{-1} and 602 cm^{-1} designate the bending band of the SO_4^{-2} ion. A narrow peak at 1385 cm^{-1} could be related to nitrates. Low intensity calcite peaks are observable in the spectrum as well.

Conclusions

The performed analyses have showed that most encountered deterioration typology among the analyzed samples, is the one of biological origin, more specifically that caused by the presence of **lichens.** Lichens represent the most often organism found on stone monuments exposed outdoors.

Lichens are composite organism formed by an *algae* and/or *cyanobacteria* responsible for the photosynthesis and a *fungus* in a mutually symbiotic relationship. Very often, other fungi or bacteria are associated to this symbiotic organism. The vegetative body part of the lichens is called thallus, and it is mainly composed by fungal hyphae. In dolomitic and other carbonates, the hyphae of some fungi, are able to penetrate the calcite crystals not only along the planes of the crystals, but also transversely, digging into the stone surface. Such lichens are able to dissolve actively the carbonate matrix for several millimeters to, exceptionally, more than a

centimeter. The principal weathering mechanisms that have been proposed as responsible for carbonate degradation caused by lichens, is their respiration and secretion of organic acids and ligands. However, the ability of lichens to modify their substratum and to contribute to the formation of new minerals, has rarely been studied.

Lichens are generally very sensitive to atmospheric pollution like sulfur dioxide and nitric oxide that they tend to disappear in the most polluted areas. Some lichen species are used for environmental biomonitoring and as bio-accumulators of metals. Despite their deteriorating effect to stone, on the other lichens provide also protection to rock surfaces in presence of intensive atmospheric pollution.

By application of ultraviolet light in optical microscopy observations, depositional facies have been recognized and differences in the structure delineated in several samples, confirming an often occurrence of recrystallized grains formation in platy limestone. **Recrystallization and cementation** of previously solubilized calcium carbonate in limestone, often results in coarsening of large grains in a matrix of fine grain. Solution and deposition can lead to the formation of concretions of various types from calcite to dolomite, from different forms of silica to clay minerals. All these forms result in a modification of the physico-chemical properties of platy limestone and the compressive strength could be lowered and its resistance weakened. Carbonate solubilization could be connected to lichens' activity and it is more rapid in waters rich in CO_2.

Another aspect, specific for platy limestone and responsible for its decay as well as for its exploitation modus, is the **detachment of material along layers (lamination)**. The intensively stratified structure implies deposition of impurities in formed fissures, that occurred still in its genesis, facilitated hyphae penetration as well as deposition of solubilized calcium carbonate or other salts. The listed characteristic deterioration factors cause significant structural weakening of platy limestone, making it a building material of relatively poor quality, which partly explains its extensive use only in roof covering.

Only on the surface of sample n. 1104 Rupinpiccolo 17 a suphatic patina was found.

On the basis of the presented results, an interesting observation could be made related to the appearance of platy limestone in its most common use, the roofs. Despite the fact that being on the roof, assuring the direct washing away by the rain water, platy limestone slabs very often have a darker coloration than the walls. As demonstrated by the analysis, this color is not caused by some formed patina or deposition of atmospheric pollution, like those caused by sulphates on limestones in urban area, but by the presence of lichens. The lichens are not pervasive, or they are in a lesser extent, on the walls below the roof. This fact could be explained with the platy limestone being more suitable for lichen colonization, probably due to its higher porosity and stratified structure. In the next figures with photo taken along the Istrian territory some example of the above explained are presented.

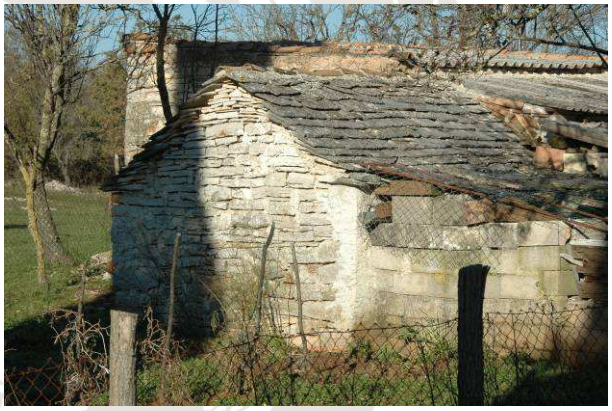

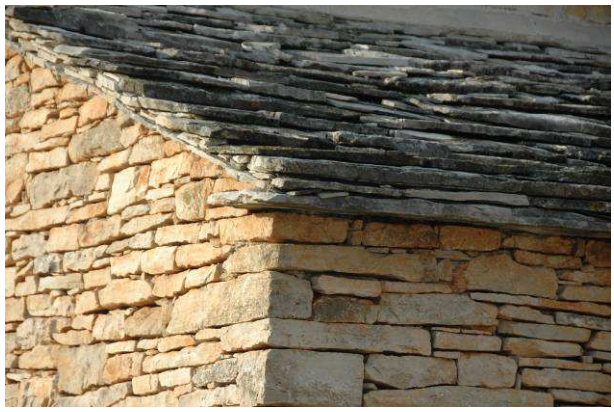

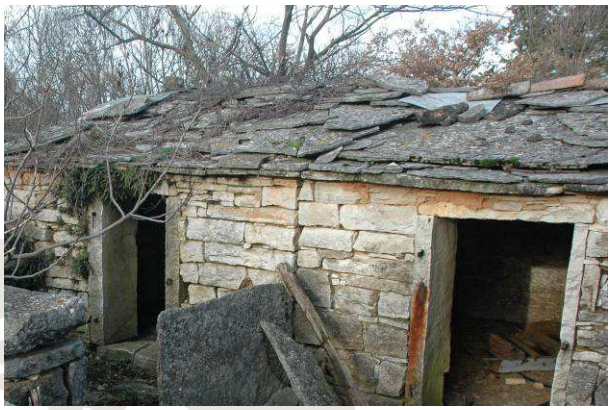


On the other hand, it is easy to recognize roofs that have been covered recently or that have been partly restored with new slabs, like can be seen in the two next figures.


Finally, the studies conducted so far about platy limestone show that it is a simple material of local production, locally extracted and used by generation who knew the properties of this material and have been used it accordingly to them. The relative poor quality of platy limestone was complemented with more often rearrangements of the roof stone slabs and replacements of the damaged ones. So it was in times when people have been building their own houses, when they actually had the time and the knowledge for that.

Mechanical properties of platy limestone

Testing of **flexural strength under constant moment** provides very useful information on the behavior of the stone material in relation to stress that for example a slab has to withstand when applied on a ventilated facade. For platy limestone slabs it is important in order to determine its maximum load especially when related to roof covering. The test was performed on 33 samples in total, but due to inappropriate form the results of some samples were omitted. The results are presented in the table below.

n.	SAMPLE ID	NAME	Country	σfM (MPa)	Quality assessment
1	3107_S4	Debelo brdo - Benkovac	Cro	19,21	excellent
2	3109_S3	3120 Benkovac PL- Benkovac (M-P)	Cro	9,57	good
3	3303_S1	3320 Vinišće (M-Bi)	Cro	17,02	excellent
4	3308_S1	3310 Milna-PL (G-R biokl.)	Cro	6,69	good
5	3308_S2	3310 Milna-PL (Bi)	Cro	13,45	very good
6	3313_S1	Prapratnica (P kalc. Lam.)	Cro	8,31	good
7	3314_S1	3330 Jelinak (P kalc.)	Cro	6,70	good
8	3502_S1	Milna - M. Stiniva (M)	Cro	9,53	good
9	3504_S1	3520 Vrboska PL (Bi)	Cro	9,72	good
10	3505_S1	3520 Vrboska PL (Bi)	Cro	7,10	good
11	3506_S1	3520 Vrboska PL	Cro	8,46	good
12	3612_S1	3630 Gornji Humac-PL (P)	Cro	7,20	good
13	3612_S2	3630 Gornji Humac-PL (P)	Cro	9,47	good
14	3612_S3	3630 Gornji Humac-PL (P)	Cro	6,51	good
15	3702_S1	Gornji Humac PL - Vis (P)	Cro	2,25	bad
16	3807_S1	Milna-PL (Vela Luka, M/W/P)	Cro	15,85	excellent
17	3813_S1	3820 Milna-PL (Žrnovo, P)	Cro	9,21	good
18	3813_S3	3820 Milna-PL (Žrnovo, P)	Cro	7,68	good
19	3905_S1	3910 Gornji Humac PL (P/M)	Cro	8,79	good
20	3917_S1	Milna PL - Nakovana (Bi)	Cro	8,31	good
21	3918_S1	Milna PL – Nakovana (M)	Cro	10,62	Very good
22	SLO7	Gabrovica	Slo	19,89	Very good
23	SLO8	Griza	Slo	8,281	good
24	SLO9	MH	Slo	3,156	bad

Categories for flexural strength:

1-5 bad

5-10 good

10-15 very good

15-20 excellent

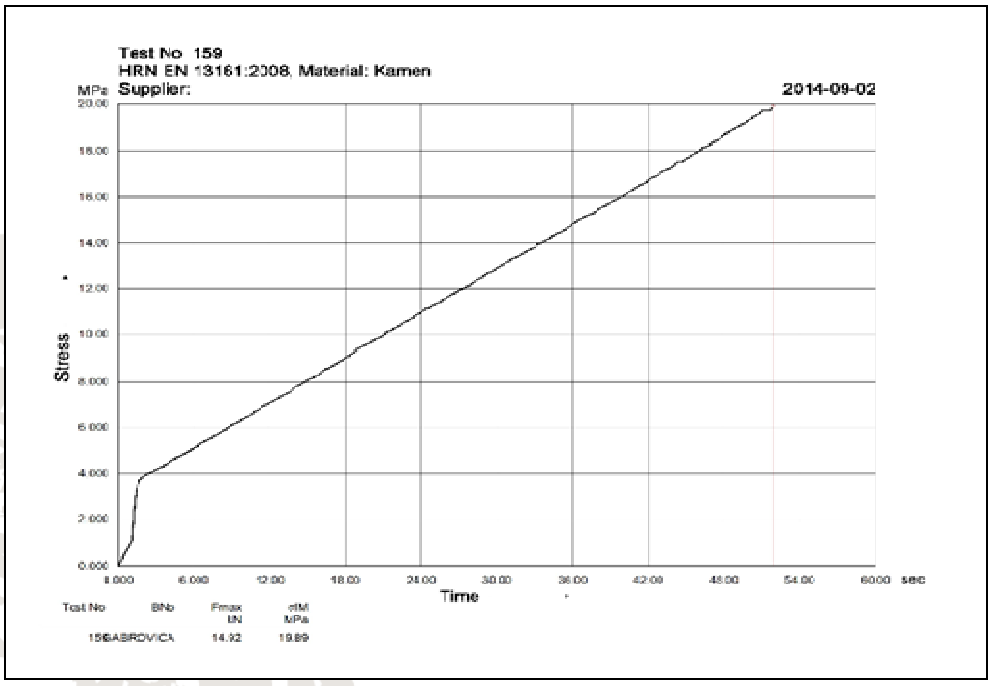

Bending test diagram of Gabrovica sample

Bending test diagram of sample *Gabrovica* shows a constant increase in stress until fracture. Fracture appeared at stress of 20 Mpa. The first part of the diagram shows the pretension of 1 MPa and a further increase of stress after which it becomes constant until fracture occurs.

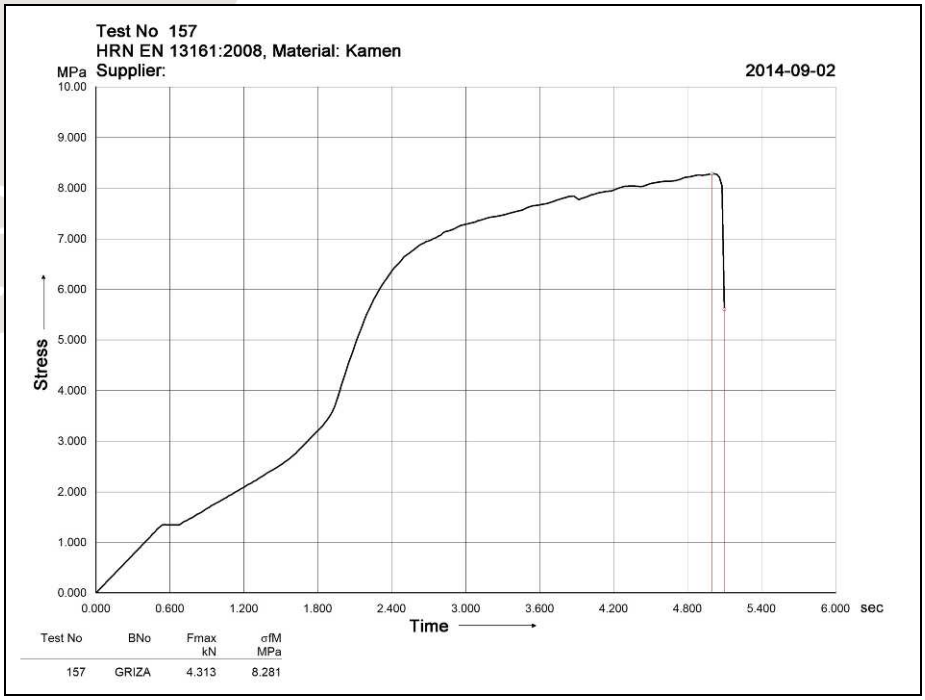

Bending test diagram of Griza sample

Diagram of the sample Griza sample shows pretension, followed by a continuous increase in stress to about 3 Mpa. After this value, there is a sudden increase of stress to about 6.5 MPa, and the continued growth up to 8 MPa when fracture occurs. This sudden increase in stress can be linked to the properties of materials. Decline of stress values after the fracture is associated with the fact that there has been no complete fracture, the fracture was slowly opening.

Griža sample before and after flexural strength testing.

The uniaxial compressive strength was performed on 4 samples. It is an important mechanical parameter which is required for many engineering projects. Uniaxial compressive strength (UCS) deals with materials' to ability to withstand axially-directed pushing forces and it is considered to be rock materials' most important mechanical property.

In the next table results of the testing are listed:

n.	Sample ID	Sample name	F max kN	Rn (MPa)	Quality assessment
1	SLO10	GABROVICA	210,00	83,98	Strong
2	SLO11	GRIZA	177,4	70,95	Strong
3	SLO12	KAZLJE	209	83,61	Strong
4	SLO13	MH	99,41	39,77	Medium strong

Categories for uniaxial compressive strength:

>250 Mpa – extremely strong

100-250 Mpa – very strong

50-100 Mpa – strong

25-50 Mpa – medium strong

5-25 Mpa – weak

1-4 Mpa – very weak

0,25-1 Mpa – extremely weak

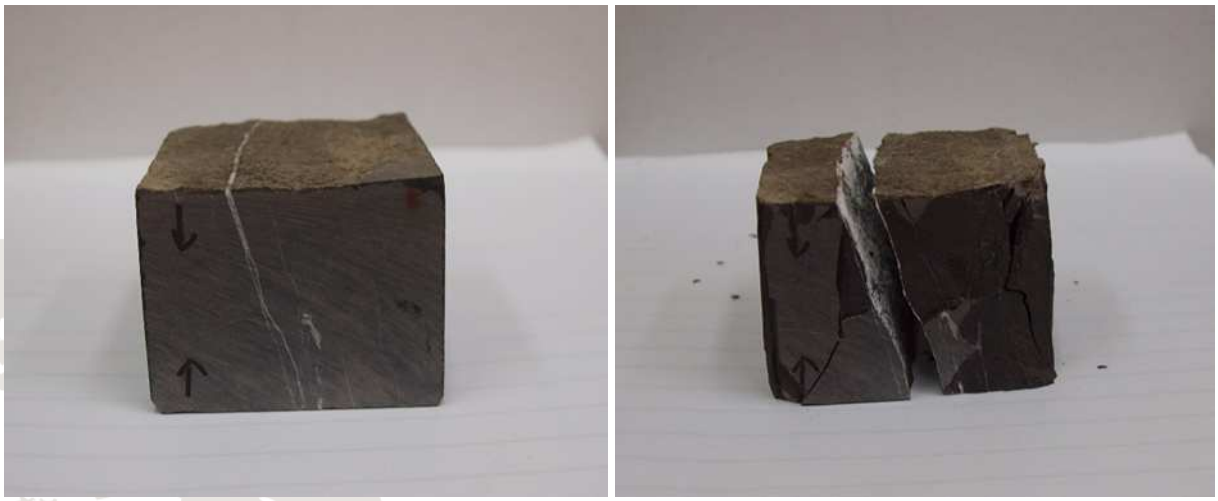

Kazlje sample before and after compressive strength testing.

The **open porosity by mercury intrusion** has been measured on 11 platy limestone samples. This parameter is one of the most important when considering the usage of stone outside, because of the effect of freezing cycles; stone with high porosity and those having little pores are more susceptible to damage caused by freezing cycles, on the other side stones with big pores, or with low porosity are more resistant. The porosity (Ø) has been defined as the fraction of the total volume of the rock occupied by "empty spaces":

$$Ø = 1 - (V_R / V_A)$$

where V_R and V_R are respectively the total apparent volume and the real volume of the sample. Mercury porosimetry is very useful for the characterization of porous materials and is widely used for stone materials, concrete, bricks etc. With this technique, pores between 500 µm and 3.5 nm can be investigated and the results provide a wide range of information: the pore size distribution, the total pore volume (the porosity), the apparent density and the specific surface area of the analyzed material. One of the limitations, on the other hand, that has to be taken into account, is that it measures the largest entrance towards a pore but not the actual inner size of a pore. The measurement performed on platy limestone samples consists of the intrusion of mercury in the pores of the samples by applying a pressure. Since mercury has very low wettability, with contact angle lower than 90°, it cannot enter the pores spontaneously. By actually measuring the pressure applied to enter the pores, information

about the dimensions of the pores are obtained. The Washburn equation explains the relation between the pressure (P), the surface tension of mercury (Y) , the contact angle (Θ) and the pores radius (r).

$$P= 2 Y\cos \Theta / r$$

In the next table, results of the porosity measurement are represented:

n.	SAMPLE ID	SAMPLE NAME	APPARENT DENSITY (g/mL)	OPEN POROSITY (%)	Total intrusion volume (mL/g)	Average pore diameter (µm)
1	ZAD 3	Medviđa, sv. Ivan Krstitelj	16,85	**38,93**	0,038	0,17
2	SLO1	Škrateljinova domačija, Divača	2,70	2,04	0,0077	0,25
3	SLO2	Pri Blaževih	2,71	**1,76**	0,0066	0,08
4	SLO4	Cerkev Marijinega vnebovzetja - Šmarje pri sežani	2,69	**1,16**	0,0044	0,92
5	ITA 1	Trebiciano 107	2,70	2,76	0,01	0,13
6	n. 1104	Rupinpiccolo 17	2,69	4,49	0,17	0,13
7	HR2	Zrenj 1 ZR1	2,72	5,00	0,19	0,06
8	HR3	Zrenj 2 ZR2	2,66	1,04	0,004	0,92
9	HR7	Laganisi	2,70	**10,34**	0,04	0,25
10	SLO14	Gabrovica	2,61	**1,54**	0,006	2,12
11	ZAD 2	Austro-hungarian sidewalk- Zadar	2,71	2,41	0,009	0,008

Below are represented the diagrams obtained within porosity measurement for samples ZAD3 and SLO9 showing various parameters.

Sample ZAD 3

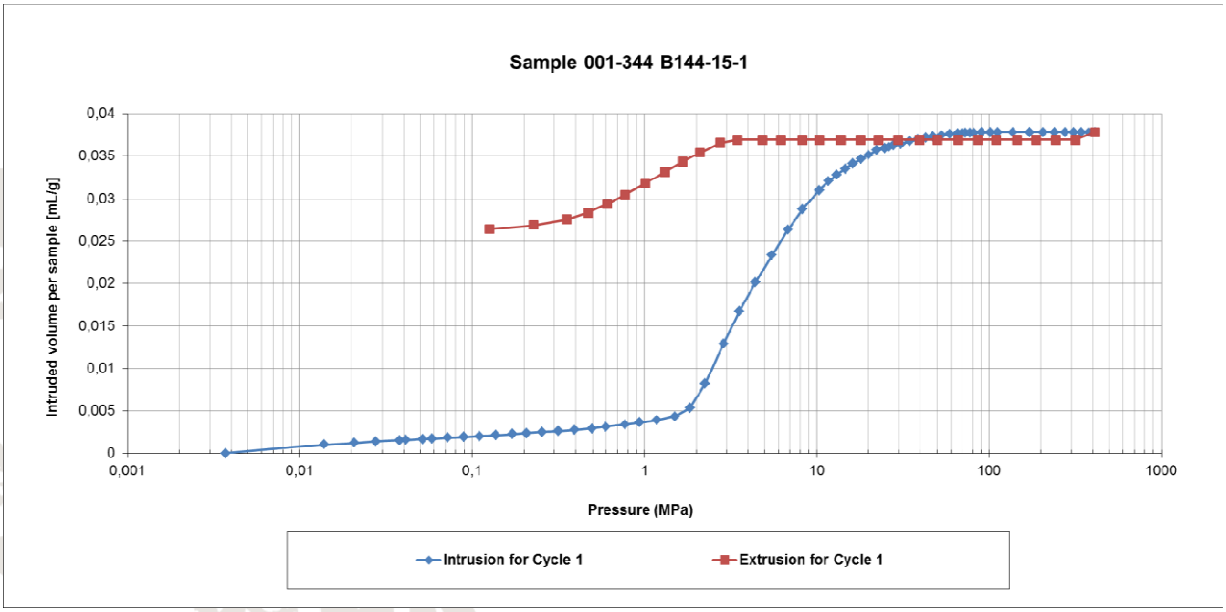
Sample 001-344 B144-15-1
Intruded volume per sample [mL/g]
0,04
0,035
0,03
0,025
0,02
0,015
0,01
0,005
0
0,001
0,01
0,1
1
10
100
1000
Pressure (MPa)
Intrusion for Cycle 1
Extrusion for Cycle 1

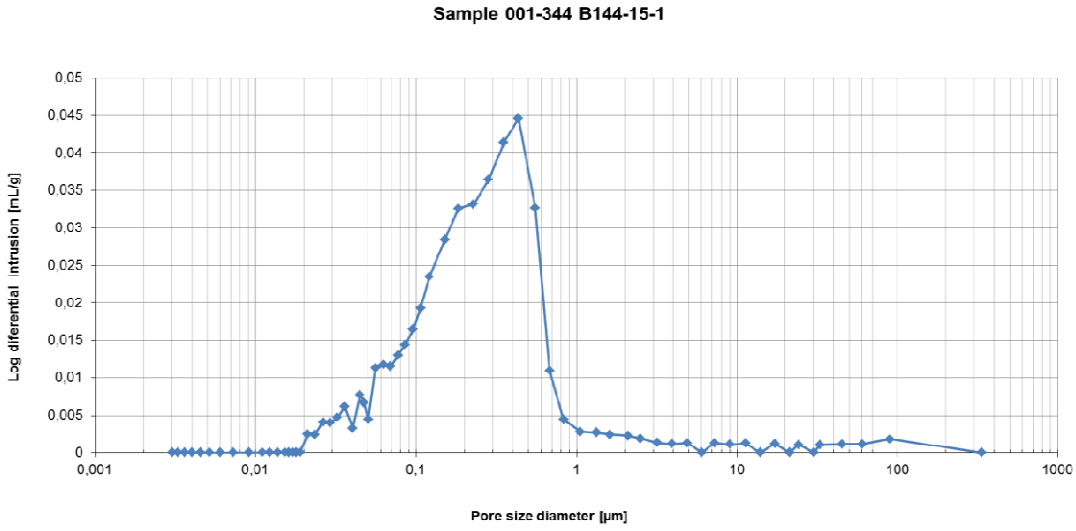
Sample 001-344 B144-15-1
Log diferential intrusion [mL/g]
0,05
0,045
0,04
0,035
0,03
0,025
0,02
0,015
0,01
0,005
0
0,001
0,01
0,1
1
10
100
1000
Pore size diameter [µm]

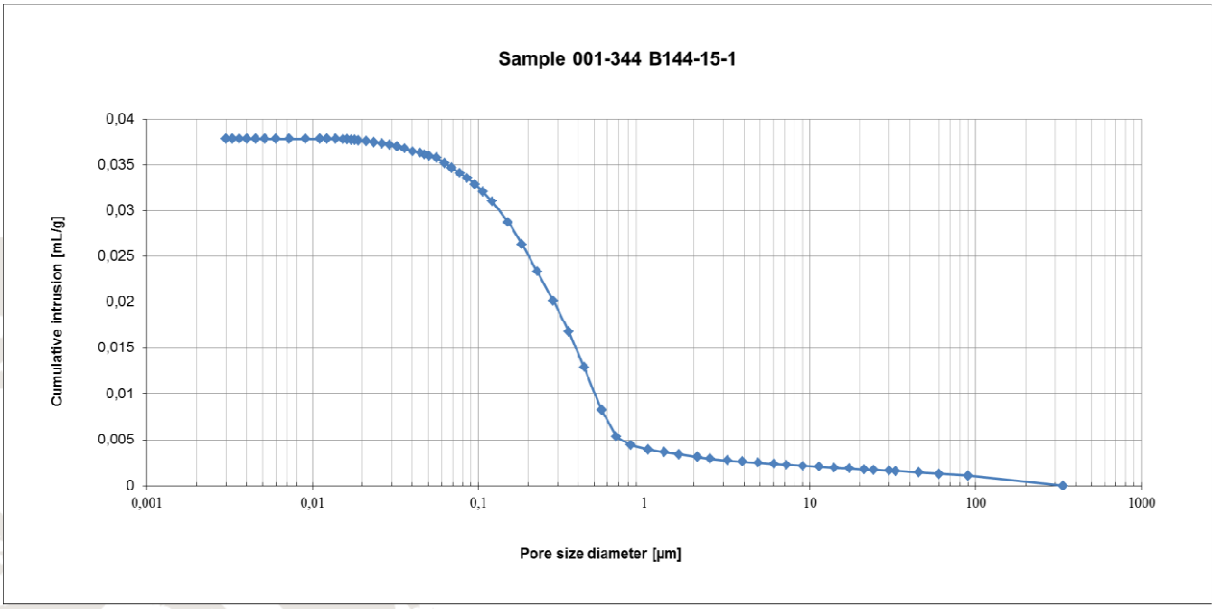
Sample 001-344 B144-15-1
Cumulative intrusion [mL/g]
0,04
0,035
0,03
0,025
0,02
0,015
0,01
0,005
0
0,001
0,01
0,1
1
10
100
1000
Pore size diameter [µm]

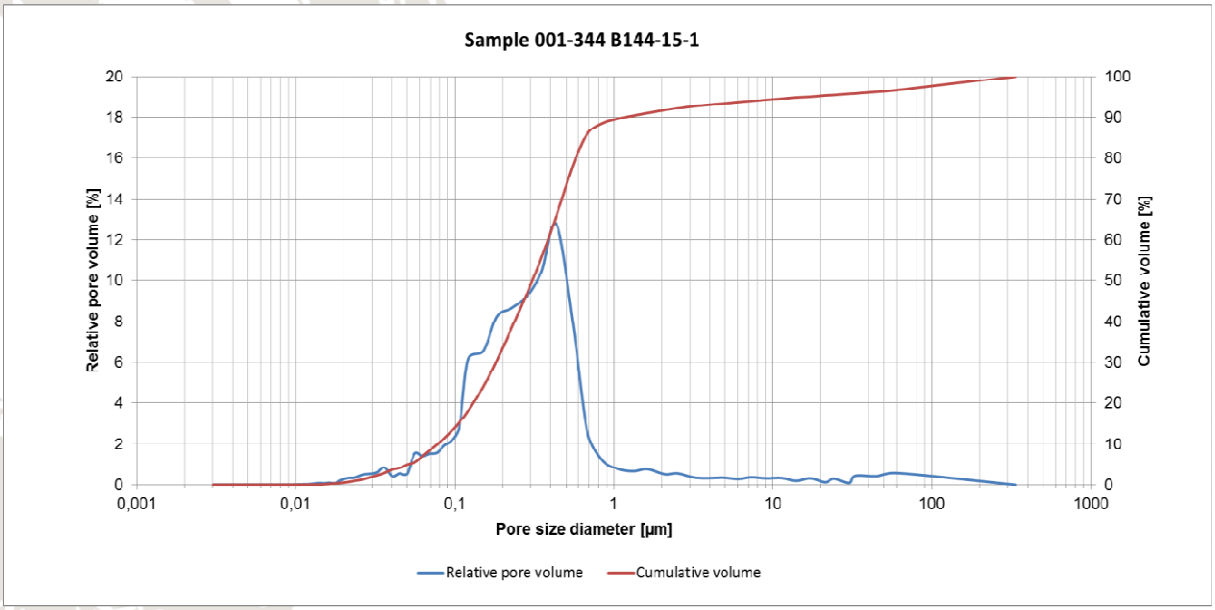
Sample 001-344 B144-15-1
Relative pore volume [%]
Cumulative volume [%]
20
18
16
14
12
10
8
6
4
2
0
100
90
80
70
60
50
40
30
20
10
0
0,001
0,01
0,1
1
10
100
1000
Pore size diameter [µm]
Relative pore volume
Cumulative volume

Sample SLO9 Gabrovica

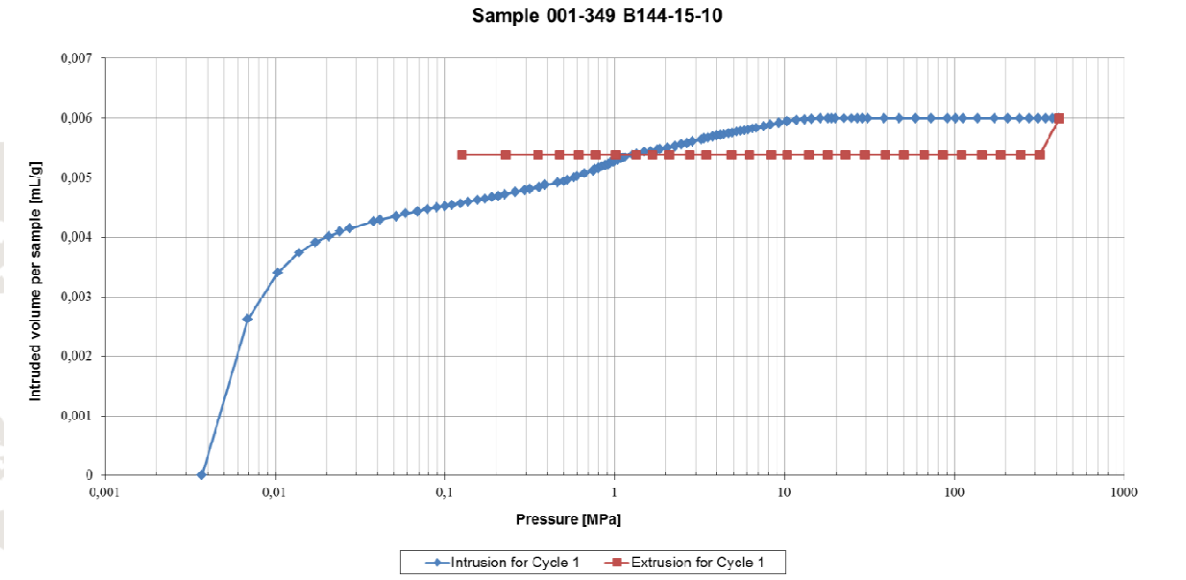

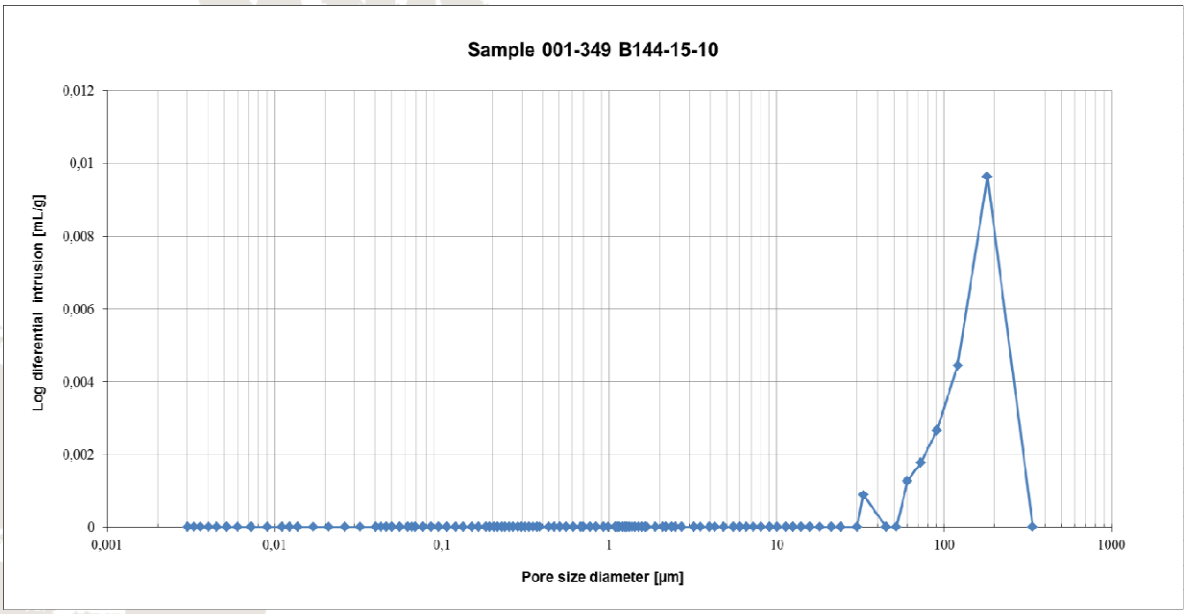

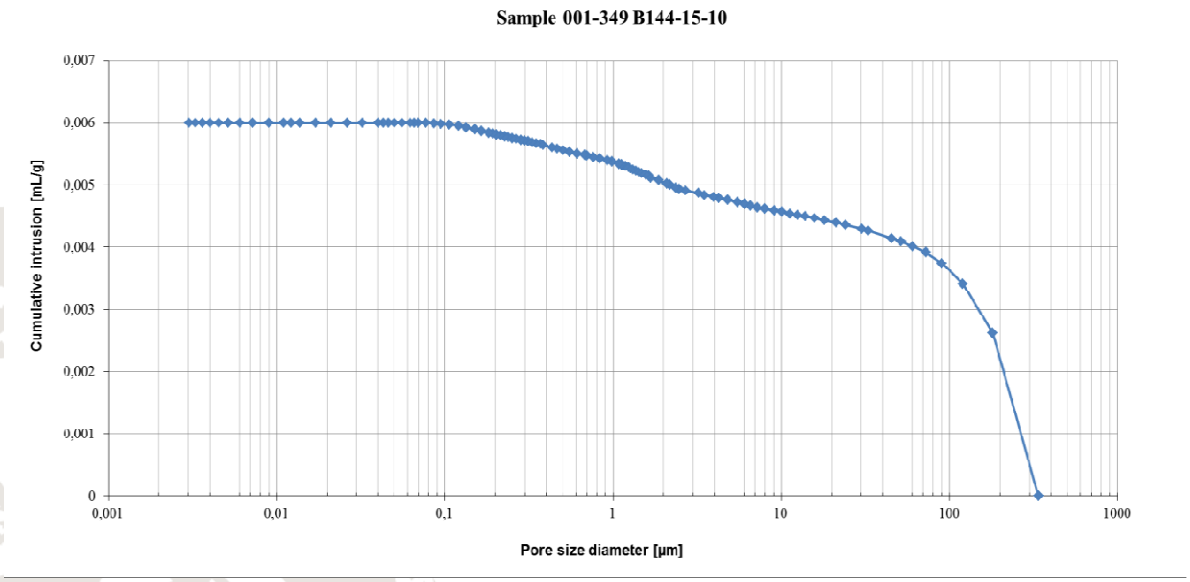

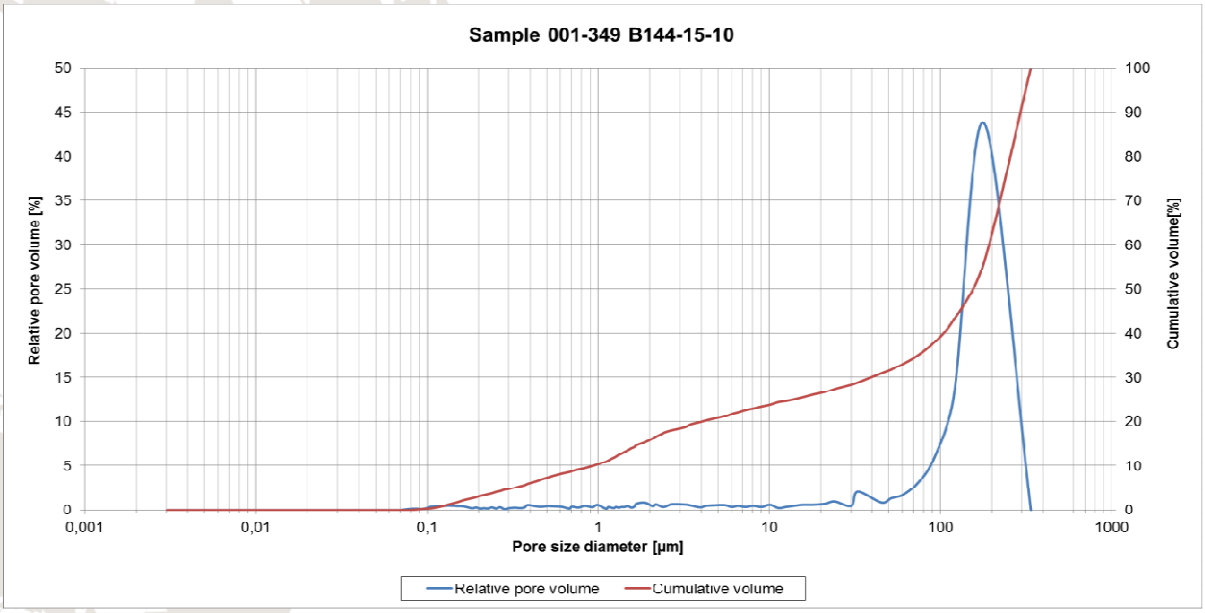

Conclusions

Significant differences among the measured values on mechanical properties of platy limestone reflect its heterogeneous structure that can be explained by its genesis, lamination and grain size. The mercury intrusion open porosity measurement has shown that the porosity varies as well. For the sample of Gabrovica SLO 14 the very low porosity can be connected to

the values obtained measuring the flexural and compressive strength showing high compactness of the mentioned stone. On the contrary, samples ZAD3 Medviđa, sv. Ivan Krstitelj, shows the most highest porosity among the analyzed samples. Microscopic analyses performed on this sample (see page 18) reflect its high porosity showing how particles of iron oxide have penetrated the bulk of the sample. Furthermore, FT-IR and SEM/EDS analyses on the mentioned sample shows that it is, together with sample ZAD 4, the only dolomitic platy limestone. The high porosity registered on this sample could be connected with dedololimitization process, wherein part of the magnesium is removed or incorporated into magnesium oxides, hydroxides, and silicates and which could increase the porosity of the limestone.

The results acquired emphasize the importance of considering the open porosity as one of the basic parameters for stone characterization and classification. The values obtained within this research are to be considered as general guidelines for quality appraisal of platy limestone, when considering to reactivate a quarry or to open new one, as well as for considering to reuse stone slabs which provenance has been defined.

Chemometric analysis of FT-IR spectra of platy limestone samples

FT-IR analysis have been performed on most of the samples studied in this research (for detailed overview see table at page 6). The bulk as well as the surface patinas of several samples have been investigated by means of FT-IR spectroscopy and the collected spectra have been used for statistical analysis, their mutual comparison and identification of a numerical value of the degree of their mutual similarity. Modern statistical methods, such as chemometric techniques, allow the processing and analysis of large quantities of data, and the clustering of results are based on various algorithms. Chemometrics is actually a branch of chemistry that studies the application of mathematical and statistical methods to chemical data by way of extracting information from complex chemical systems and applying data

processing methods such as multivariate analysis, applied mathematics and computer science in order to solve problems in chemistry, medicine, biology and chemical engineering.

Cluster analysis

A cluster analysis (Eng. *cluster* = group) is a statistical technique for grouping samples or objects, so that those within one cluster resemble more to one another with respect to those in other clusters. It is applied in various branches of science for the classification of individual units of analysis (e.g., samples or objects) based on their similarities or differences towards some their measured characteristics. For the cluster of platy limestone samples the position (wavenumber) and intensity (absorbance) of collected infrared spectra have used as measured characteristics. For the calculation of the similarities, Ward's algorithm was applied and the similarity has been based on Euclidean distance. Ward's algorithm is used whenever the most homogeneous groups want to be found. The spectra for cluster analysis were used as their first derivate and each spectrum was first processed by a correction of the baseline and a compensation of carbon dioxide peaks. The area of the spectrum where water bands occur (at 3500 -3000 cm^{-1}), were excluded of the analysis because the level of humidity in the air as well as in the samples can vary and compromise the spectra comparison.

The result of a cluster analysis is usually presented as a dendrogram, a graph showing the grouping sequence of objects (samples) according to the similarity of their FT-IR spectra, i.e., similarities in composition. On the X axis of the graph the logical distance of the clustering metrics is shown while on the Y axis the hierarchical level of aggregation is displayed.

Cluster analysis has been performed on:

1. Spectra on bulk of all samples
2. Spectra on bulk of quarry/outcrop Istrian and Slovenian samples
3. Spectra on patinas of analyzed show cases samples
4. Portions of spectra for dolomite identification on all samples

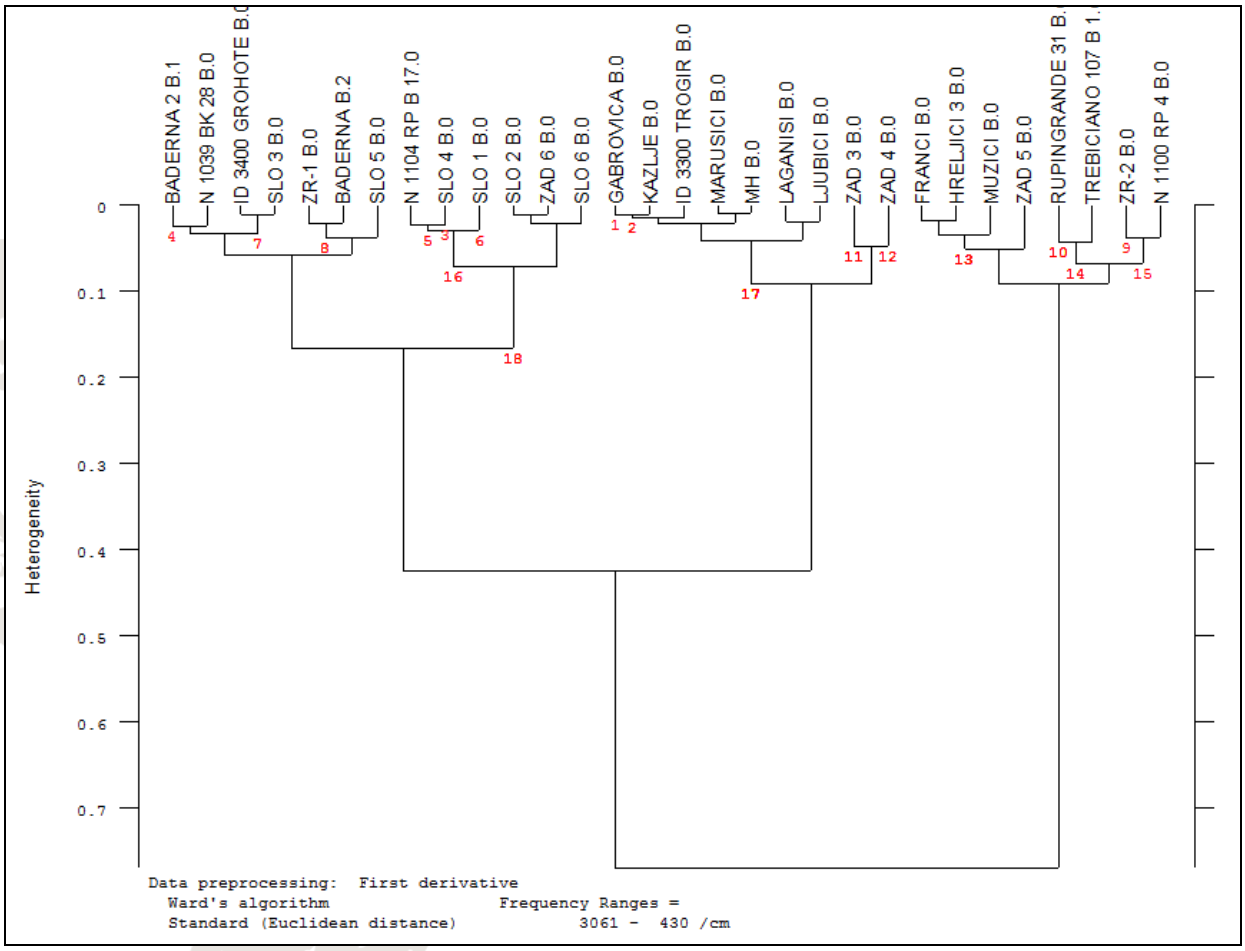

1. Dendrogram of FT-IR spectra of the bulk analyzed on all samples.

The dendrogram shows four groups where the group containing FRANICI, HRELJICI, MUZICI, ZAD 5, RUPINGRANDE 31, TREBICIANO 107, ZR 2 and 1100 RUPINPICCOLO samples, on the most right side, is the most different when compared to the others. Most of the Slovenian samples are grouped together showing their common origin, as well as ZAD 3 and ZAD 4 samples.

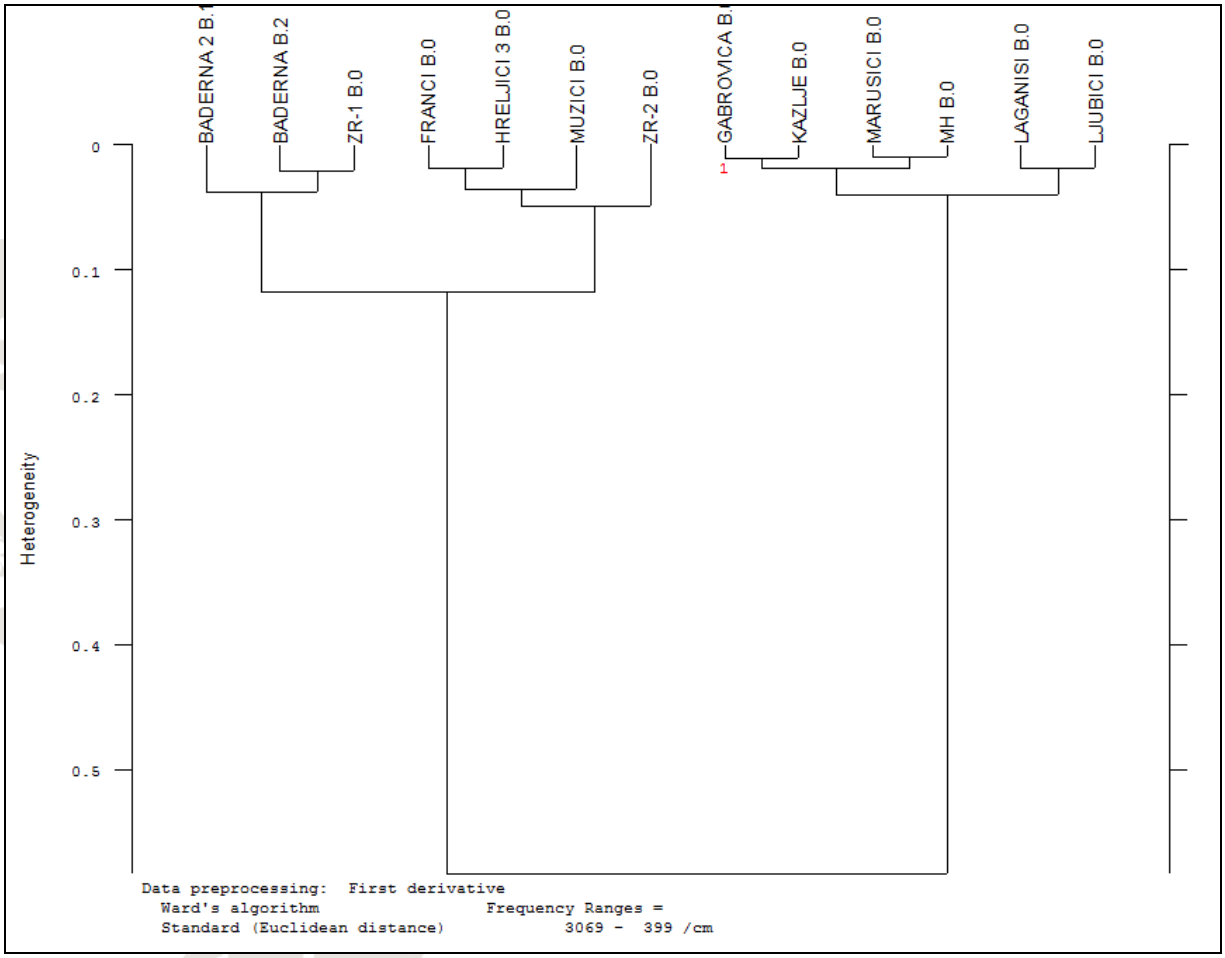

1.

2. Dendrogram of FT-IR spectra of the bulk analyzed on quarry/outcrop Istrian and Slovenian samples.

The graph shows a clear separation of the samples into two group, the first showing more heterogeneity the second and containing the two BADERNA and ZR samples as well as HRELJICI, MUZICI and FRANCI samples. The other group, the one on right side, regroup all Slovenian samples and three Croatian most similar to them: MARUSICI, LAGANISI and LJUBICI.

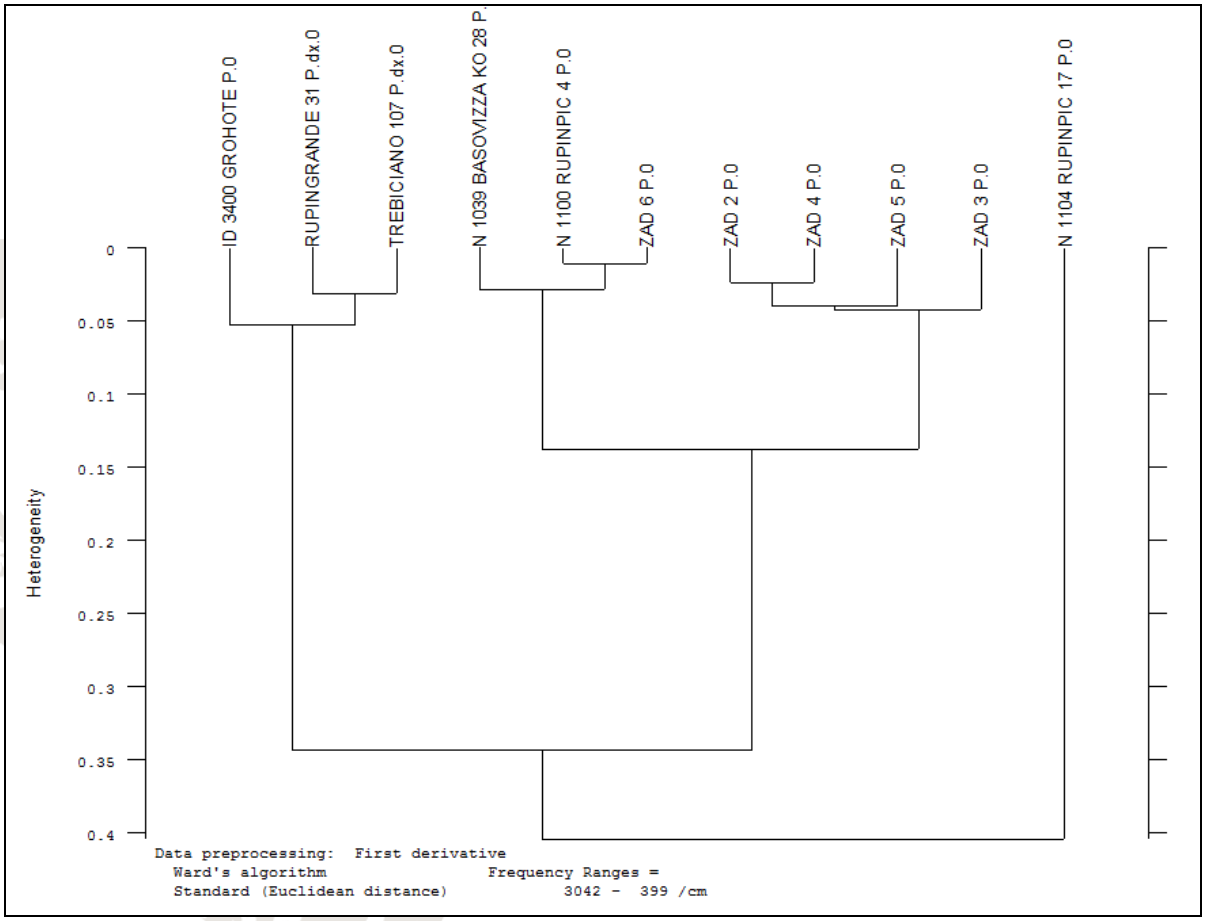

3. Dendrogram of FT-IR spectra of the patinas analyzed on show cases samples (samples from Italia and Croatia)

The dendrogram shows four main groups formed among the patina samples. The division partly reflects samples origin and partly the composition. ZAD 2, ZAD 4 and ZAD 5 are samples belonging to the church of sv. Ivan in Medviđa (near Zadar), while sample ZAD 2 was taken from an austro-hungarian sidewalk in Zadar. Sample ZAD 6 was taken from a quarry at the island Dugi Otok and shows similar composition as Italian samples of n. 1039 Basovizza – Kosovel and n.1100 Rupinpiccolo 4. A group comsed by sample taken in Grohote – Ruića dvor from Šolta island, sample and sample Trebiciano 107 and Rupingrande 31. Sample n. 1104 Rupinpiccolo 17 forms a separate group, as previously presented it is the only patina sample which formed by gypsum and which differs entirely from the rest of the patina samples analyzed.

Since some dolomite samples were found (samples ZAD 3and ZAD 4) a dendrogram was made using the spectrum area were dolomite bands are present (740 – 700 cm^{-1}) in order to find out if other dolomitic platy limestone samples are present.

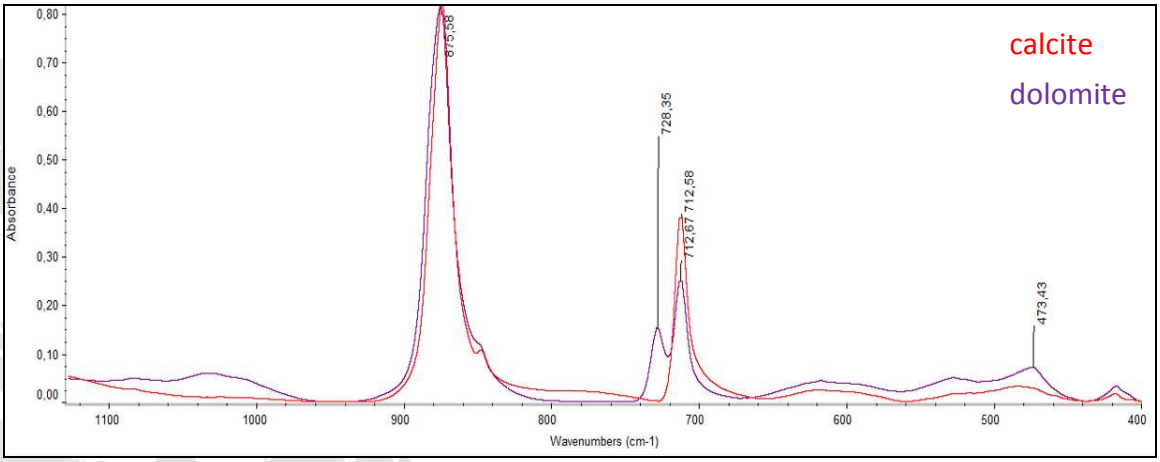

Part of the FT-IR spectrum were dolomite peaks are observable (728-730 cm^{-1}).

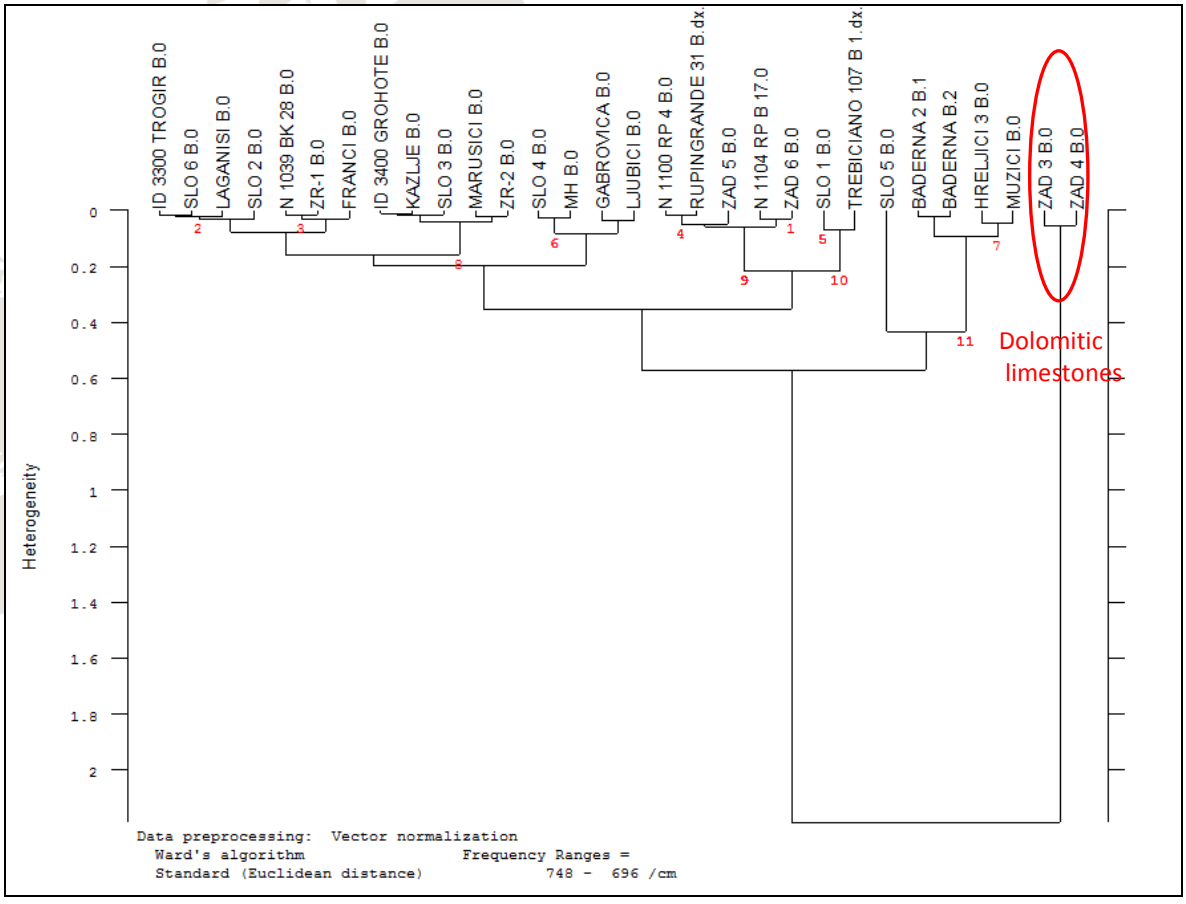

4. Dendrogram of dolomite bands of FT-IR spectra of bulk of all samples.

The graph shows clear separation of the two dolomitic limestone samples, ZAD 3 and ZAD 4, indicating that no other samples containing dolomite are present among the studied samples.

Conclusions

Cluster analysis have shown differences among samples from different zones, in the case of the superficial patinas it could be related to the environment and lichen typology, while in the case of stone spectra, a classification on the basis of the lithology would be useful to made first in order to find out if the clustering is related to it. The cluster analysis has shown that no other dolomitic limestone samples are present except ZAD3 and ZAD4.

References

- Amoroso G., Trattato di scienza della conservazione dei monumenti, Alinea, Firenze, 2002.
- Caneva G., Nugari M.P., Salvadori O., La biologia vegetale per i beni culturali, Nardini, Firenze, 2002.
- Hoek E., Brown E., Practical estimates of rock mass strength, *International Journal of Rock Mechanics and Mining Sciences*, Vol 34, No 8, 1997.
- Reed S.J.B., Electron microprobe analysis and scanning electron microscopy in geology, Cambridge University Press, 2005.

Equipment list

- Optical microscope Axio Imager M2m Carl Zeiss
- Scanning electron microscope FEG Quanta 250 FEI
- FT-IR Spectrometer Tensor 27 Bruker
- FT-IR Microscope Hyperion 1000 Bruker
- Static universal testing machine MESSPHYSIK BETA 250
- Softwer for IR spectra processing Opus 7 Bruker
- Porosimeter Hg AutoPore IV 9510

Acknowledgements

We thank the Department for Materials of the Slovenian National Building and Civil Engineering Institute in Ljubljana, PhD Mateja Golež and geologist Mateja Štefančić for the analysis of the open porosity.